MAGNETOHYDRODYNAMIC AND GASDYNAMIC THEORIES FOR PLANETARY BOW WAVES

by

John R. Spreiter
Division of Applied Mechanics
Stanford University
Stanford, CA 94305

and

Stephen S. Stahara
RM Associates, Inc.
3738 Mt. Diablo Blvd., Suite 200
Lafayette, CA 94549

ABSTRACT

A bow wave has been observed in the solar wind upstream of each of the six planets visited by spacecraft. The observed properties of these bow waves and the associated plasma flows are outlined, and those features identified that can be described by a continuum magnetohydrodynamic flow theory as opposed to a more detailed multicomponent particle and field plasma theory. The primary objectives of this paper are to provide an account of the fundamental concepts and current status of the magnetohydrodynamic and gas dynamic theories for solar wind flow past planetary bodies. This includes a critical examination of (a) the fundamental assumptions of the theories, (b) the various simplifying approximations introduced to obtain tractable mathematical problems, (c) the limitations they impose on the results, and (d) the relationship between the results of the simpler gas dynamic-frozen field theory and the more accurate but less completely worked out magnetohydrodynamic theory.

Representative results of the various theories are presented and compared. A number of deficiencies, ambiguities, and suggestions for improvements are discussed, and several significant extensions of the theory required to provide comparable results for all planets, their satellites, and comets are noted. The paper concludes with some remarks about anticipated trends in the future development and application of the theory and a description of a number of applications and extensions currently under development.

INTRODUCTION

Direct observations have established the presence of a bow shock wave upstream of each of the innermost six planets of the Solar System. These bow waves form in the solar wind plasma, which flows past the planets at supersonic speeds carrying solar plasma and magnetic fields away from the Sun, and define with certain exceptions the upstream boundary of the region influenced by the presence of the planetary body. It is the purpose of this paper to review the quantitative magnetohydrodynamic and gasdynamic theories for calculating the properties of these bow waves and their associated flow and magnetic fields.

The principal features of these flows are as follows. Hot plasma of the solar corona accelerates to supersonic speeds within a few solar radii of the Sun and flows outward through the Solar System. Because of its large scale and high electrical conductivity, this plasma carries the embedded solar magnetic field with it, distorting it as it proceeds, and generally forming a spiral magnetic field configuration as a result of the combined action of the outward flow of the plasma and the rotation of the Sun. At the orbit of Earth, the free-stream velocity v_∞ may be less than 300 km s^{-1} or greater than 1500 km s^{-1}, the proton number density N_{p_∞} may occasionally be less than 1 cm^{-3} or as high as 100 cm^{-3}, the proton temperature T_{p_∞} may be less than 50,000 K or as much as 500,000 K, and the magnetic field $\underset{\sim}{B}_\infty$ may be less than 1 nT or as much as 50 nT. The ion composition is primarily protons, i.e., ionized hydrogen atoms; with from 5 to 20 percent of helium and other ions. There is also an equal number of electrons, and their temperatures are

usually several times greater than that of the ions. The solar wind flow approaches the Earth within a few degrees of the direction to the Sun, with the aberration due to the planet's orbital motion providing a substantial part of the deviation. The interplanetary magnetic field direction is particularly variable, with the greatest predominance being approximately in the plane of the ecliptic with an angle to the Sun-Earth line of approximately 45°, and directed about equally either toward or away from the Sun.

Figure 1 illustrates the nature of the resulting flow about the Earth and other major obstacles in the Solar System in barest outline. The Earth's magnetic field, being relatively strong, dominates the plasma in an extended region surrounding the Earth to form the magnetosphere. This region is bounded by the magnetopause, a relatively thin layer in which electrical currents flow in such a way as to bound the magnetospheric magnetic field on one side and the rapidly flowing solar wind plasma and magnetic field on the other. The solar wind plasma experiences considerable difficulty in trying to cross the magnetopause, and with some exceptions is excluded from the magnetosphere and forced to flow around the magnetopause much as though it were an impenetrable obstacle. The solar wind flow approaches the planet at speeds of the order of 5 to 10 times the fastest wave propagation speeds involving the ion motions, and decelerates abruptly through a bow shock wave much as air does as it approaches a blunt-nosed obstacle at supersonic speeds. Near the nose of this bow wave, the flow is slowed to subsonic speeds, and turned to begin its flow around the magnetopause. It accelerates as it flows, and attains supersonic speeds

as it proceeds toward the flanks about as sketched. For representative conditions in the solar wind, the geocentric distance to the magnetopause nose is about 10 Earth radii, and that to the bow wave nose is about 3.5 Earth radii more.

It is apparent that many features of this flow resemble those of familiar supersonic gasdynamic flow past a blunt-nosed obstacle such as a round-nosed bullet or a re-entry space vehicle. But gasdynamics alone is not sufficient to describe other important features of the flow, such as the formation of the magnetospheric obstacle itself, that depend on the effects of a magnetic field in a highly conducting plasma. The simplest theory that is capable of representing the main features of these flows is thus magnetohydrodynamics of a compressible highly conducting plasma.

Although it is clearly established that magnetohydrodynamics can provide a remarkably good prediction of many features of these flows, it should be noted that this theory is not only complicated and far from completely worked out, but also fundamentally incapable of describing a number of other important features of the interaction. These include waves and energetic particles that sometimes propagate upstream from the bow wave along the interplanetary magnetic field, the differing nature of the magnetic field jumps across the bow wave depending on the angle between the incident interplanetary magnetic field and the shock normal, and the nonMaxwellian character of the proton velocity distributions. Analysis and prediction of such properties of these flows requires use of multi-component plasma theory as opposed to the single-fluid

magnetohydrodynamic theory under discussion in this paper; and is the subject of a number of other papers at this conference.

The Earth may serve as a prototype for discussing planetary bow shock waves and their associated flow fields, but there are also notable differences amongst the planets as outlined in Figure 1. These stem from differences in the planetary magnetic fields and atmosphere, and from changes in the solar wind with distance from the Sun. As for the solar wind, the velocity remains virtually the same from the orbit of Mercury to beyond Saturn, the temperature, density, and magnetic field all decrease with distance from the Sun, and the sonic and Alfvên Mach numbers of the flow incident upon the planets remain much greater than one; but the planetary properties differ quite markedly. Compared to the Earth, which is essentially a magnetic obstacle in the solar wind, Mercury has such a weak magnetic field and tenuous atmosphere that the distance r_o to the nose of the magnetopause is only about 1.5 times the radius r_p of the planet; whereas Jupiter and Saturn have such large magnetic fields that the ratio r_o/r_p has values of about 70 and 22 respectively. The Earth's magnetopause is approximately axisymmetric about a line through the Earth's center and parallel to the free-stream direction; whereas the magnetopause of Jupiter, and perhaps of Saturn, is flattened significantly toward the equatorial plane of the planet, probably because of its rapid rotation and large size. Venus, which formerly seemed so much like a sister planet of Earth but is now known to be very different in many respects, has virtually no detectable magnetic field, but does have a sufficiently dense ionosphere to withstand the solar wind and form an obstacle having a shape as

illustrated. In recognition that the boundary of the flowing solar wind bounds the ionosphere and not the magnetic field, it is called the ionopause. Its nose is only a few hundred kilometers above the planet's surface, and the nose of the bow wave is about a third of a planetary radius above that. The case of Mars remains uncertain because of the scarcity of observational evidence and the possibility that the location of the magnetoionopause can be accounted for by either a magnetic field or an ionospheric interaction. It is probably impossible to reach a definitive conclusion with the available magnetometer data, but other evidence indicates that there is only a small range of possibilities for the magnetic field that is compatible with the interpretation that Mars acts like a magnetic obstacle. If the magnetic field were substantially larger than the proposed values, the magnetosphere would be noticeably larger. If the magnetic field were substantially smaller than suggested, it would have negligible effect on the location of the magnetoionopause and the bow wave, and the obstacle would be clearly ionospheric.

While not a planetary body, it is of interest to comment on the case of the Moon, whose environment has been explored extensively with plasma probes and magnetometers. Its interaction with the solar wind is quite different from that of the planets. Having neither an atmosphere nor significant magnetic field, the Moon is unable to stop the approach of the solar wind until it is absorbed at the lunar surface. The solar wind thus flows unimpeded into the sunward surface of the Moon, and leaves a cavity in the solar wind extending downstream from the night side. Instead of forming a bow shock wave upstream of the Moon, a trailing expansion Mach wave fan extends from the vicinity of the lunar

terminator as illustrated through which the solar wind plasma is first turned toward the axis to begin to fill in the cavity.

Still another class of related objects in the Solar System for which similar questions are being addressed are comets. At this writing, no measurements have been made in situ at comets, but several spacecraft are already launched on their courses to rendezvous with comets in the near future. There is considerable uncertainty about the precise nature of the interaction, but the general consensus is that the situation is as illustrated in Figure 1. The comet nucleus is a source of gas and particles that melt or evaporate off as the comet travels along the more sunward part of its trajectory. These particles, emitted as neutrals, become ionized as they are exposed to sunlight and the passing solar wind particles, and in effect appear to suddenly materialize in the ionized gas flow the moment they become ionized. This simulates addition (or subtraction) of mass, momentum, and energy in the flow; thereby requiring further fundamental considerations in the formulation of the theoretical model. If the ionization occurs sufficiently rapidly and near the cometary nucleus, the flow field may resemble that of the planets with an ionopause that separates most of the cometary material from the solar wind. If the ionization extends over a substantially larger region, the approaching solar wind flow may be altered considerably, even to the extent that there might be no bow wave whatsoever as the mass-momentum-energy addition slows and heats the oncoming plasma so as to gradually change the supersonic flow to subsonic.

Finally, there are the natural satellites or moons of the other planets. Not a great deal is known about the flows about these objects, although it is evident that a number of statements can be made on the basis of their environment, sometimes in the solar wind upstream of the planetary bow wave, and sometimes in the planetary magnetoionosphere or the intervening magnetosheath flow; and also on their own atmospheric properties. From the standpoint of magnetohydrodynamic and gasdynamic theories of planetary bow waves, the differences among the various planetary flows are to some degree secondary as they are concerned more with the specification of appropriate boundary conditions than with the governing physical laws and equations. The remainder of this paper will concentrate on providing an account of the theoretical formulation and results of a number of mathematical models for these flows, and on outlining the various approximations that have been introduced to surmount the almost intractable computational problems posed by the magnetohydrodynamic model.

MAGNETOHYDRODYNAMIC THEORY FOR PLANETARY BOW WAVE FLOWS

The objective for theoretical studies of planetary bow wave flows is to predict the bow wave location and the properties in the magnetoionosheath region of the associated flow field given the properties of the incident solar wind plasma and the planetary body. The simplest theoretical model that can provide the salient features of these flows is that provided by magnetohydrodynamics of a compressible highly conducting perfect gas. This theory, which has been gradually

developed over the last forty or fifty years represents a combination of single fluid, continuum gasdynamics, and Faraday electricity and magnetism, i.e., Maxwell's displacement current is omitted on the basis of its smallness in appropriate applications. This theory is most frequently presented in its perfect dissipationless form, but it is advantageous for the present discussion to include the dissipative terms representing effects of viscosity, electrical resistance, and thermal conduction. These terms will be written in the usual way (see e.g., Landau and Lifshitz, 1960, or Jeffrey, 1966) with scalar coefficients for first and second viscosity μ and ζ, electrical conductivity σ, and thermal conductivity k; but it should be recognized that the transport properties of a nearly collisionless plasma with embedded magnetic field may be highly anisotropic with very different values parallel and perpendicular to the magnetic field. These considerations lead to the following set of partial differential equations for the pressure P, density ρ, temperature T, velocity $\underset{\sim}{v}$, magnetic field $\underset{\sim}{B}$, and entropy s involving the universal gas constant $R = 8.31 \times 10^7$ ergs $gm^{-1}K^{-1}$, the mean molecular mass $\bar{m}$ of the gas in atomic units, and the gravitational potential Φ and constant $G = 6.67 \times 10^{-8}$ dyne cm^2 gm^{-2}; and in which the independent variables are the time t and space coordinates $\underset{\sim}{x}$ of an inertial system.

Perfect gas

$$P = \rho RT/\bar{m} \tag{1}$$

Conservation laws

Mass

$$\frac{\partial \rho}{\partial t} + \frac{\partial}{\partial x_k}(\rho v_k) = 0 \tag{2}$$

Momentum

$$\frac{\partial}{\partial t}(\rho v_i) + \frac{\partial \pi_{ik}}{\partial x_k} = 0 \tag{3}$$

where

$$\pi_{ik} = \rho v_i v_k + P\delta_{ik} - \frac{B_i B_k}{4\pi} + \frac{B^2}{8\pi}\delta_{ik} + \frac{g_i g_k}{4\pi G} - \frac{g^2}{8\pi G} - \sigma'_{ik} \tag{4}$$

$$g_i = -\frac{\partial}{\partial x_i}\Phi \ , \ \sigma'_{ik} = \mu\left(\frac{\partial v_i}{\partial x_k} + \frac{\partial v_k}{\partial x_i} - \frac{2}{3}\delta_{ik}\frac{\partial v_\ell}{\partial x_\ell} + \zeta\delta_{ik}\frac{\partial v_\ell}{\partial x_\ell}\right) \tag{5}$$

Energy

$$\frac{\partial}{\partial t}\left(\frac{\rho v^2}{2} + \rho e + \rho\Phi + \frac{B^2}{8\pi}\right) + \operatorname{div} \underset{\sim}{q} = 0 \tag{6}$$

where

$$\underset{\sim}{q} = \rho \underset{\sim}{v}\left(\frac{v^2}{2} + e + \frac{P}{\rho} + \Phi\right) + \frac{1}{4\pi}\underset{\sim}{B} \times (\underset{\sim}{v} \times \underset{\sim}{B})$$

$$- \frac{c^2}{16\pi^2\sigma}\underset{\sim}{B} \times \operatorname{curl} \underset{\sim}{B} - \underset{\sim}{v} \cdot \underset{\approx}{\sigma'} - k\underset{\sim}{\nabla} T \tag{7}$$

or the Heat Transfer Equation

$$\rho T \frac{Ds}{Dt} = \sigma'_{ik}\frac{\partial v_i}{\partial x_k} + \operatorname{div}(k\underset{\sim}{\nabla}T) + \frac{c^2}{16\pi^2\sigma}(\operatorname{curl} \underset{\sim}{B})^2 = \operatorname{div}(k\underset{\sim}{\nabla}T)$$

$$+ \frac{\mu}{2}\left(\frac{\partial v_i}{\partial x_k} + \frac{\partial v_k}{\partial x_i} - \frac{2}{3}\delta_{ik}\frac{\partial v_\ell}{\partial x_\ell}\right)^2 + \zeta(\operatorname{div} \underset{\sim}{v})^2 + \frac{c^2}{16\pi^2\sigma}(\operatorname{curl} \underset{\sim}{B})^2 \tag{8}$$

and the Faraday (preMaxwell) Electricity and Magnetism Equations

$$\frac{\partial \underset{\sim}{B}}{\partial t} = \underset{\sim}{curl}\ (\underset{\sim}{v} \times \underset{\sim}{B}) + \frac{c^2}{4\pi\sigma} \nabla^2 \underset{\sim}{B}\ , \quad \text{div}\ \underset{\sim}{B} = 0 \tag{9}$$

In these equations π_{ik} and σ'_{ik} are the momemtum flux and viscous stress tensors, g_i is the acceleration of gravity, δ_{ik} is the Kronecker delta function, $\underset{\sim}{q}$ is the energy flux vector, and $e = c_v T$ is the internal energy. Other relations not explicitly used in the above equations, but that are useful in the discussion that follows are for the enthalpy $h = e + P/\rho = C_p T$ and for the difference $c_p - c_v = R/\bar{m}$ and ratio $c_p/c_v = \gamma$ of the specific heats at constant pressure and volume.

To these equations must be added appropriate boundary conditions to represent properties of the incident solar wind and the planetary body. These include ρ_∞, T_∞, $\underset{\sim}{v}_\infty$, and $\underset{\sim}{B}_\infty$ in the incident solar wind and ρ_0, T_0, $\underset{\sim}{v}_0$, $\underset{\sim}{B}_0$, Φ_0, and ion composition at some magnetoionosphere reference level between the magnetoionopause and the planetary surface.

The difficulties presented in the solution of these equations are so great that neither analytic nor numerical solutions have yet been obtained for realistic three-dimensional boundary conditions representative of a planetary application. These difficulties arise from several sources. First of all, the equations are nonlinear and the dissipative terms that contain the highest order derivatives in each of the differential equations are all multiplied by small coefficients. The shock waves and boundary and current layers that appear in the course of the solution are thus finite but thin regions of rapid variation at locations that cannot be specified in advance, but must be

found as part of the solution. Their adequate treatment requires the use of either fine spatial grids over extended regions or fine adaptive grids in the vicinity of the surface; or the acceptance of poor resolution of the solution in these regions of rapid variations at best, and widespread contamination of the solution at worst. Use of fine spatial grids requires small time steps in unsteady simulations, or very many iterations to converge a steady flow simulation. All of these factors contribute to the substantial computational requirements arising from the sheer magnitude of the problem. Eight quantities ρ, T, $\underset{\sim}{v}$, and $\underset{\sim}{B}$ must be calculated at every grid point. For reasonable resolution of the total 3-D interaction region, there would be a minimum of say 100 x 100 x 100 = 10^6 grid points not allowing for extra grids in the vicinity of shock waves, boundary layers, etc., and hundreds to thousands of iterations or time steps required to converge to a steady state solution from an assumed set of boundary and initial conditions. Obviously, the calculation of solutions will remain costly for some time, and we believe it will be many years before solutions of these equations will become inexpensive enough for extensive routine use in the analysis and interpretation of space observations.

However, advances in computational capabilities are still increasing at a rapid pace, approximately doubling every 7 years according to Chapman (1979), due almost equally to advances in computers and in numerical methods. We may enquire at this point, therefore, as to what might be anticipated from the solutions of these equations if they could be attained. First, we believe these solutions would indeed provide good predictions of the bow wave location and the large-scale

features of the associated flow. Shock waves and magnetoionopause regions would have finite thickness, and magnetic merging and reconnection would occur at the magnetoionopause. There would also be extensive heating and rarefaction at these boundary regions, particularly those of the ionopause type, with the possible formation of magnetic barrier regions of high magnetic field separating the solar wind and ionospheric plasmas.

We believe that these predictions would be correct qualitatively, but the quantitative predictions would be unreliable because of inadequancies of the scalar transport coefficients. As noted previously (Spreiter, 1976), the expressions developed for nonmagnetized plasmas are highly inappropriate. For example, the widely used expression $\mu = 10^{-16} T^{5/2} = 0.469\ v_{t_p} \rho \ell_d$ g cm^{-1} s^{-1} for the viscosity of fully-ionized hydrogen having a representative value of 22 for the Coulomb logarithm, and in which T is the temperature in K, v_{t_p} is the thermal velocity of the protons, ρ is the density, and ℓ_d is the effective mean free path for cumulative deflection of 90° by Coulomb interactions, leads to a Reynolds number $R_e = \rho v D/\mu$ of only 0.002 when the number density of protons $N_p = 10$ cm^{-3}, $T = 10^5$ K, and the radius of the Earth 6.37×10^8 cm is taken for D. Such a value for R_e is not at all indicative of an aerodynamic-like solar-wind flow past the Earth; but is more typical of a small ball sinking through tar! Use of such a value for μ would lead to the prediction of enormously thick boundary layers and shock waves, completely different from those observed.

There is no dilemma, however, since the particles were assumed in the derivation to travel in straight lines between collisions which, even in the more conservative sense of cumulative small Coulomb deflections, are indicated to be separated by mean distances of the order of half an astronomical unit when the above-stated conditions are applied. This is obviously grossly inappropriate for planetary applications which involve phenomena of much smaller scale.

Part of the answer to this apparent deficiency is provided by the fact that the presence of a magnetic field in the solar wind prevents the particles from traveling in straight lines between collisions, and causes them to spiral along the moving magnetic field lines. This reduces the transport transverse to the field lines approximately as the square of the ratio of the gyroradius of the protons to the distance ℓ_d. If a representative value of 1.4×10^{-6} is used for this ratio, corresponding to a magnetic field of 5 nT, the Reynolds number in the example cited above would increase to 9×10^8. Such a value is of the order of that encountered in ordinary aerodynamics, and is consistent with the presence of relatively thin shock waves and magnetoionopause surfaces and the generally good agreement between observations and the results of dissipationless fluid theories.

However, all is not that simple. The magnetic field does not reduce the transport coefficients equally in all directions; in fact, it does not reduce the values for transport parallel to the field lines at all. The dissipative part of the associated model is thus highly anisotropic. The direction of the anisotropy, moreover, depends on the

magnetic field, and hence also the flow, and cannot be specified in advance. Since there is at present virtually no theoretical development for the behavior of such a fluid for any application, the space scientist studying these features of the flow in terms of an anisotropic dissipative fluid is faced with the task of achieving major theoretical advances or, as is more often the case, being satisfied with hopefully describing what he thinks will happen in qualitative terms based on analogy with the known behavior of isotropic fluids. In view of the extreme anisotropy of the solar-wind plasma and the fact that the Coulomb deflection times upon which the analysis is based are much longer than the times required for solar-wind particles to traverse the significant part of a planetary flow field, it is evident that considerable caution should be exercised in relying on such descriptions. It is, moreover, quite possible that this particle approach to transport coefficients may be only marginally relevant to the actual dissipative processes; and that the significant mechanisms are associated more with larger scale eddying and turbulent features of the flow as in many analogous situations with boundary layers in ordinary fluid mechanics.

Finally, we may anticipate that the presence of time derivatives and nonlinear convective terms in equations (2) through (9) almost certainly leads to fluctuations (turbulence?) in the solutions, particularly downstream of shock waves and with increasing distance from the nose along the magnetoionopause. These may, in fact, be correct

predictions, but their presence and small scale introduces additional complications in the numerical solution that probably exceed by a substantial margin present computational capabilities to resolve .

Actual solution of the dissipative magnetohydrodynamic equations for planetary flows is still in its infancy (see Walker (1983) for a recent review). At the present time, about the only solution that has been worked out by using physically realistic, as opposed to numerical, dissipation is that of Brackbill (1982) illustrated in Figure 2. This is for unsteady two-dimensional, as opposed to three-dimensional, flow about a magnetic dipole, and is intended to demonstrate the sequence of events which follow the southward turning of the interplanetary magnetic field. The time units are Earth radii divided by the solar wind speed. As the southward field reaches the dayside magnetopause, reconnection begins at $t = 35$. Reconnection in the tail occurs when the rotational discontinuity reaches the nightside at $t = 45$. A magnetic bubble forms in the tail (n) which propagates down the tail. Earthward of the reconnection region, tail field lines first are stretched out (n_i) and then snap back to a more dipolar configuration as tail reconnection begins. To verify that it is physical resistivity and not numerical resistivity that is responsible for the tail reconnection, Brackbill also ran his code with the electrical resistivity set to zero. In this case, reconnection occurs on the dayside because of numerical resistivity, but none occurs on the nightside. It should be recognized that these and other unsteady two-dimensional models are fundamentally deficient in that there can be no return flow around the Earth back to the dayside. Therefore magnetic flux must be returned to the dayside

artificially. In addition, questions of stability may have very different results in two and three dimensions. To illustrate, nobody would marvel at a tight-rope walker in a two-dimensional world! On the other hand, the appeal of two-dimensional models is great in numerical simulations because of the substantial reduction in the number of numerical values involved. For the example cited above with 100 grid cells in each direction the reduction is from 8×10^6 to 6×10^4 values required to define conditions at any step in the calculation.

DISSIPATIONLESS MAGNETOHYDRODYNAMIC THEORY FOR PLANETARY BOW WAVE FLOWS

Because of the difficulties noted above, most analyses and discussions of planetary bow wave flows have been based on the dissipationless magnetohydrodynamic theory. This avoids altogether the uncertainties associated with the proper form of the dissipative terms, and all the mathematical difficulties associated with the thin, but finite, regions of rapid variations representing the bow wave, magnetoionopause, etc. The equations defining this theory are just equations (1) through (9) with all the terms involving μ, ζ, k, and σ set equal to zero.

Let us examine the consequences of omitting the dissipative terms. There is no diffusion of vorticity, heat, or magnetic field; there is no magnetic merging nor recombination, and magnetically separated regions can occur. The magnetic flux through a circuit that moves with

the fluid is constant; giving rise to the "frozen field" concept. Entropy, and hence P/ρ^{γ}, is constant for a fluid element, and thus constant along a streamline for a steady flow, except when it crosses a shock wave. Since the amount of entropy increase varies along the bow wave, the entropy differs from one streamline to the next. Such a flow is often called isentropic, but not homentropic. This entropy condition reduces the number of dependent variables from 8 to 7 at each grid point. Shock waves, boundary layers, and current sheets used to represent the bow wave, magnetoionopause, and other thin layers become mathematical discontinuity surfaces of zero thickness across which the plasma properties change discontinuously in definite ways governed by the conservation laws. This requires use in the numerical solution of either shock fitting techniques, probably with adaptive grids; or shock capturing methods with artificial viscosity, thermal, and electrical conductivities, either explicit or numerical, which thicken the discontinuity surfaces over several grid spacings. It is anticipated that most of the differences between these solutions and the corresponding dissipative ones are confined to the regions near these discontinuities; and that there is probably little change in most of the large-scale features of the predicted flow and magnetic field properties. Finally, we remark that the dissipationless equations are still difficult and costly to solve; and that very few solutions have actually been determined for realistic three dimensional flows at this time.

There are, however, a number of definite and exact solutions of these equations for simpler boundary and initial conditions that are fundamental to both the qualitative interpretation of planetary bow wave

flows and the establishment of quantitative predictive models based on the dissipationless magnetohydrodynamic theory. Foremost is the normal propagation speed C_n of a plane wave. In gasdynamics, this is equal to the speed of sound C_S and the resulting expression $C_S = (\gamma RT/\bar{m})^{1/2}$ follows directly from the dissipationless forms of equations (1) through (9) with the magnetic field $\underset{\sim}{B}$ set to zero. This speed is the same in all directions, and can be represented in a planar cross section by the circle shown in the upper left of Figure 3 in which C_S for a plane sound wave is illustrated as a function of angle Θ between the wave normal and an arbitrary coordinate axis. Sound waves depend on the compressibility of the medium, and do not occur in an idealized incompressible fluid. In magnetohydrodynamics, however, wave propagation can occur even in an incompressible conducting fluid. Such waves are the Alfvén waves, and the diagram in the upper right of Figure 3 illustrates how the normal propagation speed C_{n_A} of such a plane wave varies with direction such that $C_{n_A} = C_A \cos \Theta$, where $C_A = (B^2/(4\pi\rho))^{1/2}$ is the Alfvén speed and Θ is the angle between the wave normal and the magnetic field. The two lobes in this figure are thus circles osculating at the origin with their line of centers along the direction of the magnetic field. Plane Alfvén waves can propagate in any direction, except exactly normal to the magnetic field, but it can be deduced from the properties illustrated that the disturbance created by a point source will propagate only along the direction of the magnetic field and with the Alfvén speed C_A. Values for C_S and C_A for fully ionized hydrogen plasma are shown in Figure 3, from which it can be concluded that both C_S and C_A have values of about 25 to 50 km s^{-1} for conditions representative of those in the solar wind at the orbit of Earth.

The propagation speeds of a magnetohydrodynamic plane wave in a dissipationless perfect gas are substantially more complex than either of the two limiting cases just discussed. There are, first of all, three distinct wave modes each with propagation speeds varying with angle Θ. Of these, the rotational wave is simplest to discuss. It has exactly the same propagation speed and properties as the Alfvén wave for an incompressible fluid. The other two plane wave modes, with

$$C_n = \pm \frac{1}{2}\{C_S^2 + C_A^2 \pm [(C_S^2 + C_A^2)^2 - 4C_S^2 C_A^2 \cos^2\theta]^{1/2}\}^{1/2} \qquad (10)$$

are called the fast and slow waves because their propagation speeds are greater or less than that of the rotational wave. The fast wave, which has a plus sign before the inner square root, is of greater interest because it determines the region of influence and dependence in the solution, and in the flow it represents. Its normal velocity C_{n_f} varies from a maximum of $(C_S^2 + C_A^2)^{1/2}$ in the direction perpendicular to the magnetic field to a minimum equal to the larger of C_S or C_A in the direction of the magnetic field. From the two bottom diagrams of Figure 3, it may be concluded that the gasdynamic sound speed C_S approximates reasonably the magnetohydrodynamic fast wave speed for $C_S > C_A$, but poorly for $C_S < C_A$.

For steady flows with velocity in excess of the fast wave speed, the Mach cones from an infinitesimal point disturbance are of prime interest. Their traces in the plane of the $\underset{\sim}{v}$ and $\underset{\sim}{B}$ vectors may be constructed either from the curves at the bottom of Figure 3, which are called Friedrichs I diagrams, by constructing the envelope curves called

the Friedrichs II diagrams and drawing tangents from the end of the velocity vector terminating at the origin (see e.g., Jeffrey (1966)); or directly from the Friedrichs I diagrams by the procedure illustrated in Figure 4 (Spreiter et al., 1966b). In the latter, a circle is drawn with the velocity vector as a diameter, and the Mach cone is determined by the straight line from the end of the velocity vector to the intersection of the circle and a C_n curve of the Friedrichs I diagram. There are thus, in general, three Mach cones, each associated with one of the three kinds of waves; and they are appropriately called the fast, slow, and rotational Mach cones. They correspond to the single Mach cone of gasdynamics shown in the upper right of Figure 4, which makes an angle $\omega = \arcsin (M_S^{-1})$ with the velocity vector. The magnetohydrodynamic Mach angles depend not only on M_S and M_A, but on the angle Θ. To illustrate the latter effect, four limiting cases are presented in the lower parts of Figure 4. For a given M_S and M_A, the maximum and minimum Mach cone angles are given by $\omega_{max} = \arcsin (M_S^{-2} + M_A^{-2})^{1/2}$ and the larger of $\omega_{min} = \arcsin (M_S^{-1})$ or $\omega_{min} = \arcsin (M_A^{-1})$. For $\underset{\sim}{B}$ parallel to $\underset{\sim}{y}$, $\omega_{\parallel} = \arcsin \{[(M_S^2 + M_A^2 - 1)/(M_S^2 + M_A^2)]^{1/2}\}$, and for $\underset{\sim}{B}$ perpendicular to $\underset{\sim}{y}$, $\omega_{\perp} = \arcsin\{(\{M_S^2 + M_A^2 + 1 + [(M_S^2 + M_A^2 + 1)^2 - 4M_S^2 M_A^2]^{1/2}\}/(2M_S^2 M_A^2))^{1/2}\}$. Lack of appreciation of these differences is widespread in the space research literature.

The wave speed and Mach cone diagrams of Figures 3 and 4 are for infinitesimal disturbances, and are therefore not appropriate for dealing with the finite disturbances associated with the planetary bow wave and any other shock waves that may develop in the flow. These are governed by the magnetohydrodynamic discontinuity relations, which

follow directly from the conservation laws and auxiliary relations of equations (1) through (9). With the unit vectors normal and tangential to the discontinuity surface defined by n and t, the differences between any quantity Q downstream and upstream of the discontinuity designated by $[Q] = Q_2 - Q_1$, and $\tilde{v}_n = v_{n_{flow}} - v_{n_{disc}}$, which for steady flow is $\tilde{v}_n = v_{n_{flow}}$, the conservation laws for mass, momentum, and energy are

$$[\rho \tilde{v}_n] = 0 \tag{11}$$

$$[\rho \tilde{v}_n \underset{\sim}{v} + (P + \frac{B^2}{8\pi})\,\hat{n} - \frac{B_n \underset{\sim}{B}_t}{4\pi}] = 0 \tag{12}$$

$$[\rho \tilde{v}_n \,(e + \frac{P}{\rho} + \frac{v^2}{2} + \frac{B^2}{4\pi\rho}) - v_{n_{disc}}\,(P + \frac{B^2}{8\pi}) - \frac{B_n(\underset{\sim}{v}\cdot\underset{\sim}{B})}{4\pi}] = 0 \tag{13}$$

These must be solved together with the Faraday magnetic jump equations

$$[\underset{\sim}{B}_t \tilde{v}_n - B_n \underset{\sim}{v}_t] = 0 \quad , \quad [B_n] = 0 \tag{14}$$

and the auxiliary condition for entropy $[s] \geq 0$. In gasdynamics, these conditions with $\underset{\sim}{B}$ set to zero completely determine the shock jump relations; but in magnetohydrodynamics an additional condition is required. It is the evolutionary condition (see, for example, Jeffrey and Taniuti (1964)), which states in essence that there must be a mechanism by which a succession of infinitesimal waves can evolve into a finite discontinuity. This distinction does not have to be made in gasdynamics because the entropy condition implies the evolutionary condition and conversely; but this is not so in magnetohydrodynamics. In the latter, the evolutionary condition implies the entropy condition, but the entropy condition does not imply the evolutionary condition;

and both must be satisfied. An example of a situation in which the entropy condition, but not the evolutionary condition is satisfied is the case in which the shock normal is parallel to the magnetic field and M_S and M_A are within certain ranges. Theory indicates that a finite magnetohydrodynamic shock wave cannot evolve from an accumulation of infinitesimal waves; and observational evidence indicates that a well defined shock wave may indeed fail to develop under such conditions.

Solutions of equations (11) through (14) show that five types of discontinuity surfaces may occur in dissipationless magnetohydrodynamic flows. They may be classified as two boundary types for which $\tilde{v}_n = v_{n_{flow}} - v_{n_{disc}} = 0$, namely

tangential discontinuities

$$B_n = 0,\ [\underset{\sim}{v}_t] \neq 0,\ [\underset{\sim}{B}_t] \neq 0,\ [\rho] \neq 0,\ [P + B^2/8\pi] = 0 \tag{15}$$

contact discontinuities

$$B_n \neq 0,\ [\underset{\sim}{v}] = [\underset{\sim}{B}] = [P] = 0,\ [\rho] \neq 0 \tag{16}$$

and three shock wave types for which $\tilde{v}_n \neq 0$, namely

rotational or Alfven shock waves

$$\tilde{v}_n = \tilde{v}_{n_r} = \pm B_n/(4\pi\rho)^{1/2}\ ,\quad [\underset{\sim}{v}_t] = [\underset{\sim}{B}_t/(4\pi\rho)^{1/2}] \tag{17}$$

$$[\rho] = [P] = [v_n] = [v^2] = [B^2] = [B_n] = 0$$

fast shock waves

$$\rho\tilde{v}_n > \rho\tilde{v}_{n_r}\ ,\ [\rho] > 0\ ,\ [P] > 0\ ,\ [B_n] = 0\ ,\ [B^2] > 0 \tag{18}$$

slow shock waves

$$\rho\tilde{v}_n < \rho\tilde{v}_{n_r}\ ,\ [\rho] > 0\ ,\ [P] > 0\ ,\ [B_n] = 0\ ,\ [B^2] < 0 \tag{19}$$

All types may be anticipated in planetary flow fields if there are sufficient fluctuations in the solar wind or planetary flow boundaries. They may also be improperly induced by growing perturbations in a numerical solution of the dissipationless equations, unless controlled by artificial viscosity and conductivities.

More explicitly, a planetary bow wave must normally be a fast shock wave because ρv_n of the incident solar wind exceeds ρv_{n_r} by a considerable margin over the forward part of the bow wave; and the magnetoicnopause must normally be a tangential discontinuity in order to separate the solar wind and planetary magnetic fields and plasmas. The outermost Mach wave of the Moon must be a fast Mach wave, and the boundary between the flowing solar wind plasma and the lunar downstream cavity might be either a tangential or a contact discontinuity. In addition, all of these types of discontinuities can occur in the solar wind as a result of interactions of plasmas with differing speed and properties.

The most completely worked out solution for dissipationless magnetohydrodynamic flow past a planetary obstacle is that of Spreiter and Rizzi (1974) for the special case of an axisymmetric obstacle in a flow in which $\underset{\sim}{B}$ is parallel to $\underset{\sim}{v}$ in the incident solar wind (see also Spreiter et al., 1970) for a related application to the Moon). Under these conditions $\underset{\sim}{B} = \lambda\rho\,\underset{\sim}{v}$ everywhere; and the dissipationless magnetohydrodynamic equations can be transformed into those of gasdynamics by introduction of new variables

$$\underset{\sim}{v}^* = \underset{\sim}{v}[1-\lambda^2\rho/(4\pi)] \ , \ \rho^* = \rho[1-\lambda^2\rho/(4\pi)]^{-1},$$

$$p^* = p + B^2/(8\pi) \ , \ S^* = S \ ,$$

$$h^* = h + [\lambda^2\rho/(4\pi)][1-\lambda^2\rho/(4\pi)] \ , \ h = e + P/\rho \qquad (20)$$

in which

$$\lambda^2\rho/(4\pi) = M_A^{-2} = (\rho/\rho_\infty)\, M_{A_\infty}^{-2} \qquad (21)$$

except that the equation of state $P = \rho RT/\bar{m}$ is replaced by a rather complicated relation that corresponds to no real gas. These pseudogasdynamic equations can be solved using the methods developed for ordinary gasdynamics to produce the results displayed in Figure 5. They show, for a given axisymmetric obstacle shape and fixed $M_{S_\infty} = 10$ and $\gamma = 5/3$, the location of the bow wave for selected M_{A_∞} between 2.5 and 20. The conclusion to be gained from these results is that the magnetohydrodynamic bow wave locations are virtually independent of M_{A_∞} for values greater than about 10, and are practically identical with those of gasdynamics in which all effects of the magnetic field are disregarded. They also show that for small M_{A_∞} the bow wave flares out more at the flanks, but approaches the obstacle closer near the nose. From this, it is evident that attempts to represent the combined effects of M_{S_∞} and M_{A_∞} by an "equivalent value" for M_{S_∞} to be used in a gasdynamic model cannot succeed. In gasdynamics there is a monotonic relationship between M_{S_∞} and distance to the bow wave in all directions from the obstacle. If M_{S_∞} is diminished, the bow wave moves farther from the obstacle everywhere. There is no way that an equivalent Mach number can be found that will simultaneously move the flanks of a gasdynamics bow wave farther outward and the nose farther inward.

Solutions for non-aligned fields are much more difficult to work out than for the aligned case, and very few results are available at the present time. Among these is the solution of Wu, Walker, and Dawson (1981) for three-dimensional, steady, magnetohydrodynamic flow past a dipole magnetic field to simulate the Earth, for which constant density and pressure contours are presented in Figure 6. Although there is no magnetic field in the interplanetary plasma in their model, the results display the broad outlines of the observed flow. The results indicate a moderately defined bow wave across which conditions change approximately in accordance with the Rankine-Hugoniot jump conditions, and a poorly defined magnetopause. The locations of the magnetopause and bow wave resemble those observed in space, although it should be noted that the Mach number used in the calculations, i.e., $M_{S_\infty} = 2.5$, is substantially less than that normally observed in the solar wind upstream of the Earth's bow wave. Perhaps the least satisfactory aspect of the theory is the thickness of the bow wave and the magnetopause. The model boundaries are 4-5 Earth radii (3-4 grid spaces) thick, whereas the observed boundaries are a few hundred kilometers thick at most, and usually considerably thinner. The calculated thickness of these boundaries results from the numerical dissipation in the simulation, which erroneously spreads over several grid spacings what should be a mathematical discontinuity surface in the dissipationless theory on which the model is based. It may be anticipated on the basis of continuing rapid improvements of computers and numerical algorithms that finer grids will be used in future models, thereby providing better resolution of these regions of rapid variation. As long as numerical dissipation is used in the calculations, however, caution should be

exercised in interpreting the results, particularly those associated with real dissipative processes that may be expected to occur. Although the prediction of such features may tantalizingly resemble those actually believed to occur, it should be remembered that the associated quantitative values lack proper physical basis, and must be regarded more as suggestive than quantitative predictions.

THE GASDYNAMIC APPROXIMATION OF MAGNETOHYDRODYNAMIC PLANETARY FLOWS

In recognition of the great computational demands of full magnetohydrodynamic solutions, particularly as viewed in terms of the limited computing ability then available, an approximate theory of considerable utility was developed about two decades ago. Following on the success of purely gasdynamic calculations by Axford (1962), Kellogg (1962), and Spreiter and Jones (1963) of flow past an obstacle shape defined by the Beard (1960) and Spreiter and Briggs (1961) solutions of the classical Chapman-Ferraro theory of interaction of a collisionless stream of protons and electrons with a magnetic dipole, a more consistent approximate theory based on magnetohydrodynamics was developed by Spreiter et al. (1966a,b; 1967; 1968; 1969; and 1970a,b,c), Alksne et al. (1967, 1970), and Dryer et al. (1966, 1967). In this theory, the magnetohydrodynamic tangential discontinuity jump conditions are retained for the boundary conditions at the magnetopause, and the bow wave is identified as a fast magnetohydrodynamic shock wave, which would tend to resemble a gasdynamic shock wave for large M_{A_∞} and

for $M_{A_\infty} > M_{S_\infty}$. The key approximation is that the magnetic terms may be disregarded in the momentum and energy conservation equations on the basis of their smallness for large M_{A_∞}. The resulting equations are thus

Perfect gas

$$P = \rho RT/\bar{m} \tag{22}$$

Conservation laws

Mass

$$\frac{\partial \rho}{\partial t} + \frac{\partial}{\partial x_k}(\rho v_k) = 0 \tag{23}$$

Momentum

$$\frac{\partial(\rho v_i)}{\partial t} + \frac{\partial}{\partial x_k}\left(\rho v_i v_k + P\delta_{ik} + \frac{g_i g_k}{4\pi G} - \frac{g^2}{8\pi G}\right) = 0 \tag{24}$$

Energy

$$\frac{\partial}{\partial t}\left(\frac{\rho v^2}{2} + \rho e + \rho\Phi\right) + \operatorname{div}\left[\rho \underset{\sim}{v}\left(\frac{v^2}{2} + e + \frac{p}{\rho} + \Phi\right)\right] = 0 \tag{25}$$

and the Faraday Electricity and Magnetism Equations

$$\frac{\partial \underset{\sim}{B}}{\partial t} = \operatorname{curl}\left(\underset{\sim}{v} \times \underset{\sim}{B}\right), \quad \operatorname{div} \underset{\sim}{B} = 0 \tag{26}$$

The heat transfer equation degenerates to $Ds/Dt = 0$, which indicates that the entropy is constant along a streamline for dissipationless flow; but this relation does not apply across a shock wave because dissipation always occurs there in such a way that $[s] > 0$ with the amount of entropy augmentation depending on the incident Mach number and the angle between the shock normal and the free-stream velocity vector. In most, but not all applications, the gravitational terms involving g and Φ may be omitted.

With this approximation, the conservation equations become exactly those of gasdynamics. The magnetic field $\underset{\sim}{B}$ therefore has no influence in the solution for the pressure P, the density ρ, the temperature T, or the velocity $\underset{\sim}{v}$. The latter quantities can be solved for using the methods of gasdynamics without further consideration of the magnetic field. The Faraday magnetic equations are the same as in the dissipationless magnetohydrodynamic theory, which implies that the magnetic field is "frozen" into the flow. However, the values for $\underset{\sim}{v}$ in equation (21) are those of the gasdynamic solution. The resulting prediction for the magnetic field differs from that of an exact magnetohydrodynamic solution by an unknown amount dependent on the difference in the velocities in the two theories. This approximate separation of the magnetohydrodynamic problem into two parts, which can be solved in succession, leads to a significant reduction in computing requirements. The resulting component problems are still sufficiently complex that they have not been solved without further approximation. These difficulties are associated not only with the nonlinear and mixed elliptic-hyperbolic type of the differential equations, but also with the discontinuity surfaces that represent the bow wave and the magnetoionopause whose locations are not known a priori but must be found as part of the solution.

Problems associated with the unknown location of the magnetoionopause can be avoided to an acceptable degree over most that surface by use of an approximate relation for the pressure of the flowing solar wind on the magnetoionopause, i.e.,

$$P = K \rho_\infty v_\infty^2 \cos^2 \psi \qquad (27)$$

This serves to decouple the calculation of the magnetoionopause shape from that of the surrounding flow. In this relation, K is a constant usually equated to unity and ψ is the angle between the free-stream velocity and the exterior normal to the magnetoionopause with directions defined so that $\psi = 0$ at the magnetoionopause nose. With the proper selection of a value for K, this relation provides good results for the pressure over most of the magnetoionopause, but deterioration sets in as ψ approaches $\pi/2$. For $\psi \geq \pi/2$, equation (27) is totally inappropriate, and should not be used.

Equation (27) has two distinct origins in planetary studies. On the one hand, there is the original usage in a long series of works starting with Chapman and Ferraro (1931) and particularly Ferraro (1952) in which the relation $P = K\ m_p\ n_p\ v_\infty^2 \cos^2\psi$ is derived by considering the interaction of a collisionless stream of protons of mass m_p and number density N_p and an equal number of electrons, all with uniform initial velocity $\underset{\sim}{v}_\infty$, with a dipole magnetic field oriented normal to the flow. Depending on the assumptions, K was usually found to be either 1 or 2, although 1/2 also appears occasionally in the literature of the time. That analysis was developed from a cold particle stream viewpoint to explain how a cavity that we would now call the magnetosphere forms in a collisionless plasma stream or cloud of solar origin that sweeps past the Earth and produces a geomagnetic storm.

The second line of argument that leads to equation (27) stems from the recognition that a highly supersonic solar wind exhibiting continuum fluid-like properties is present at all times; and that one of its manifestations is the bow shock wave that forms upstream of the magnetosphere, which acts much as an impermeable obstacle in the flow. From this point of view, equation (27) may be regarded as a close approximation for high Mach number flow to the Newtonian pressure relation for hypersonic flow $P - P_\infty = K \rho_\infty v_\infty^2 \cos^2\psi$. This is usually, but not always, approximated in planetary applications by equation (27) in which P_∞ is disregarded on the basis of its relative smallness as indicated by $P_\infty = \rho_\infty v_\infty^2/(\gamma M_\infty^2)$. The constant K is determined from the Rayleigh pitot formula for the stagnation pressure for supersonic flow decelerated to rest after passing through a normal shock wave. Under these conditions, K is found to be

$$K = \left(\frac{\gamma+1}{2}\right)^{(\gamma+1)/(\gamma-1)} \frac{1}{\gamma[\gamma-(\gamma-1)/(2M_\infty^2)]^{1/(\gamma-1)}} \qquad (28)$$

For large Mach numbers, K = 0.881 for $\gamma = 5/3$ and 0.844 for $\gamma = 2$, the two most-commonly used values for the ratio of specific heats γ in planetary flow studies. In using these pressure relations, it should be observed that equation (27) is not an exact relationship within any modern formulation of planetary flow theory. The original collisionless plasma beam theory is inappropriate because it disregards completely the deflection of the flow by the bow wave and in the intervening region; and the gasdynamic derivation is approximate because the Newtonian

pressure relation is a semi-empirical relation that is not exact in any limiting case. That equation (27) does indeed lead to good results compared with an essentially exact numerical gasdynamic solution for a number of representative solar wind conditions has been shown by Spreiter et al. (1966b, 1968). It seems to us equally plausible to consider for magnetohydrodynamic applications that $K \rho_\infty v_\infty^2 \cos^2\psi$ should be equated to the sum of the gas and magnetic pressures $P+B^2/8\pi$ or $(P+B^2/8\pi)-(P_\infty+B_\infty^2/8\pi)$ rather than to P or $(P-P_\infty)$ alone as is customary.

With the latter interpretation and disregarding $P_\infty+B_\infty^2/8\pi$ as small, the tangential discontinuity boundary condition to be applied at a planetary magnetoionopause becomes

$$K\rho_\infty v_\infty^2 \cos^2\psi = (P + B^2/8\pi)_{MIP} \ , \ B_n = 0 \qquad (29)$$

where subscript MIP refers to conditions just below the magnetoionopause. This enables the calculation of (a) the magnetoionopause location, and (b) conditions in the magnetoionosphere without further consideration of the solar wind plasma flow; and (c) reduces these problems for an idealized magnetic planet to those of the classical but physically outmoded Chapman-Ferraro theory (1931).

We may summarize the specifications for such an idealized problem, and also its counterpart for a nonmagnetic planet, as follows. In either case, the normal component of the magnetic field is zero, and the solar wind pressure $K \rho_\infty v_\infty^2 \cos^2\psi$ on the magnetoionopause is balanced by the sum of the magnetic and ionospheric gas pressures on the inside of the magnetoionopause in accordance with equation (29). Inside the magnetosphere of a magnetic planet such as the Earth, the intrinsic

planetary field dominates until it is terminated by the currents flowing in the magnetopause. Other current systems are present and important in the calculation of magnetospheric processes; but, with the exception of the magnetotail current sheet which flows across the tail in approximately the geomagnetic equatorial plane, they are usually relatively unknown and unimportant, and disregarded in the calculation of the magnetopause shape and the surrounding flow. The field inside the magnetosphere is therefore just that of the intrinsic planetary field, usually approximated for the Earth by a magnetic dipole as distorted by the effects of the currents in the magnetoionopause and the tail plasma sheet. That field is calculated by solving

$$\text{div } \underset{\sim}{B} = 0 \ , \ \text{curl } \underset{\sim}{B} = 4\pi \underset{\sim}{j}/c \tag{30}$$

subject to the boundary conditions

$$K\rho_\infty v_\infty^2 \cos^2\psi = (B_t^2/8\pi)_{MP} \ , \ B_n = 0 \tag{31}$$

at the magnetopause due to a planetary magnetic dipole field

$$\underset{\sim}{B}_p = -(M_p/r^3)(\hat{\underline{\theta}} \sin\theta + \hat{r}\ 2\cos\underline{\theta}) \tag{32}$$

at the origin. In this equation, M_p is the planetary magnetic moment and r and $\underline{\theta}$ are geomagnetic radius and colatitude. In most applications $\underset{\sim}{j} = 0$ except at the magnetopause and in the tail current sheet. With neglect of the latter, the problem is exactly the Chapman-Ferraro problem.

For a nonmagnetic planet with a sufficiently dense ionosphere to stop the solar wind, the corresponding problem is specified by assuming the ionospheric pressure above some reference level P_0 can be approximated by

$$P = P_0 f(r,\theta) \ , \ \underset{\sim}{B} = 0 \tag{33}$$

within the ionosphere; and

$$K\rho_\infty v_\infty^2 \cos^2\psi = P_{IP} \tag{34}$$

at the ionopause. In the original presentation of this model (Spreiter et al., 1970a,b), the ionospheric pressure was assumed to be simply $P = P_0 \exp[-(r-r_0)/H]$ where $H = RT/\bar{m}g$ = const, i.e., a constant scale height ionosphere was assumed. Subsequently, Spreiter and Stahara (1980a,b) and Stahara et al. (1980), included the inverse square variation of the gravitational acceleration g with r, while retaining the simple assumption of a constant temperature ionosphere. With improved knowledge, as has since been acquired for Venus, the only known clearly nonmagnetic planet, refinements in the specification of $f(r,\theta)$ can obviously be made and incorporated into the calculations. We believe that little change in the ionopause shape will result, however, because the rate at which P diminishes with r is so great that only small changes in the ionopause shape will result. In other words, a nonmagnetic planet with a substantial ionosphere, such as Venus, presents a rather firm obstacle to the solar wind flow compared with a strongly magnetic planet as the Earth or Jupiter for which considerable

change in the size of the magnetosphere occurs with variations in the solar wind momentum flux $\rho_\infty v_\infty^2$.

Figure 7 illustrates the resulting shape calculated for the magnetopause associated with a magnetic dipole of magnitude and range of orientations in the solar wind resembling that of the Earth. These results are for the first-order approximation of Beard (1960) as solved by Spreiter and Briggs (1962) and Briggs and Spreiter (1963). A number of higher-order solutions have been worked out subsequently, but the results are virtually indistinguishable on the scale shown and the differences are not particularly relevant to the present discussion. (See Wu and Cole, 1982, and Wu, 1983, for recent commentary.) These results, and all others of the kind, have been based on the Chapman-Ferraro formulation of the interaction. However, they may equally be considered to be solutions of the continuum gasdynamic or even magnetohydrodynamic models to the extent that the solar wind pressure on the magnetopause can be approximated by the extended Newtonian relation of equation (29). From the latter point of view, inaccuracies in the calculated magnetopause shape may be anticipated along the magnetosphere tail and near the neutral points because the Newtonian pressure relation becomes increasingly inaccurate as ψ approaches $\pi/2$. The neutral points are of particular interest because they represent points in the idealized theory where the magnetospheric magnetic field vanishes and particle entry into the magnetosphere may occur. There is considerable evidence that such entry does indeed occur, but any quantitative prediction of conditions in the vicinity of the neutral points that uses the Newtonian pressure relation in the

boundary condition as given in equation (31) or (33) must be regarded as unreliable. The reason is that the condition $\underset{\sim}{B} = 0$ at a neutral point leads through the boundary condition to $\cos^2\psi = 0$, or $\psi = \pi/2$; but that is precisely the condition for which the Newtonian approximation clearly fails. In the Chapman-Ferraro plasma beam approach, a further deficiency is that effects of double impacts, as would occur near a neutral point when a particle grazes the magnetopause just forward of the neutral point and hits the magnetopause again just aft of the neutral point, are not considered. In the continuum gasdynamic or magnetohydrodynamic models, the presence of an indented region results in the formation of an embedded shock attached to the surface (Walters, 1966); but Spreiter and Summers (1967) pointed out that such a shock could not develop adjacent to the magnetopause. The reason is that the pressure jump across the shock wave cannot be matched with a corresponding jump in the magnetic pressure in the magnetosphere. The resolution they proposed was that the flow would separate somewhat ahead of the neutral point and then reattach downstream of the neutral point, and that the constant pressure along the intervening free streamline surface would cause a cusp-shaped plasma filled region to form. Recent magnetohydrodynamic numerical solutions of Wu (1983) support this proposal. With the cusped geometry, it is no longer required for the magnetic field to vanish at the netural point, but solar wind particles can still enter the magnetosphere near the tip of the cusp. Considerable interest has been attached to observations in these polar cusp regions in recent years, and also to the conditions in the mantle region which extends downstream from the cusped regions along the magnetopause.

From the present point of view of planetary bow waves and their associated flow fields, perhaps the main point is that there exists a well worked out body of theory for the calculation of the magnetopause shape and location, and that it has been found in a great many studies to provide a reasonably good prediction of conditions actually observed in space. This is true for both the Earth and for other planets for which data are available, provided allowance is made for the differing nature of the planetary obstacles. For example, the ionopause shape for the nonmagnetic planet Venus is axisymmetric in the theory and nearly so in observations; and there are of course no neutral point phenomena. Jupiter's magnetosphere appears to be flattened somewhat toward the equatorial plane, which is understandable in terms of the effects of its extremely large trapped particle regions and high spin rate.

To proceed with the solution of our problem, the next step is to calculate the supersonic gasdynamic flow around the magnetopause, which can at this stage be considered to be similar to an impermeable obstacle of known shape. For a nonmagnetic planet, this obstacle is axisymmetric about the line through the planet center directed along the free-stream velocity direction. For a magnetic planet, as the Earth, however, the obstacle shape is nonaxisymmetric and a decision has to be made whether or not to include the effects of the moderate departure from axisymmetry. When the original calculations were made over twenty years ago, there was no choice. Only the theory for axisymmetric flow had been developed, and even that was very new at the time. The computers and methods then available were totally inadequate for dealing with a fully three-dimensional supersonic flow past a blunt body. As a result,

a further simplification was introduced in that the magnetopause was approximated by an axisymmetric shape. This was usually, but not always, taken to be the body formed by rotating the equatorial trace of the magnetopause surface. This choice was motivated partly by that fact that most space observations for the Earth were made near the equatorial plane. Today, advances in computers and numerical methods, and recent motivation provided by the needs of the nonaxisymmetric space shuttle as opposed to the axisymmetric vehicles of the earlier era, have made available methods for calculating supersonic gasdynamic flows about nonaxisymmetric blunt objects. However, the cost in computing time rises substantially for these 3-D flows, and the errors from assuming an axisymmetric magnetopause shape are anticipated to be no larger than those from a number of other sources in the entire procedure.

Even with the assumption of an axisymmetric obstacle, the determination of the gasdynamic flow properties is the most difficult and time-consuming portion of the numerical solution of the entire planetary flow and magnetic field problem. As sketched in Figure 8, two different methods are used in the calculations; one for the nose region, where both subsonic and supersonic flows occur, and another downstream of that region, where a more computationally economical procedure can be employed since the flow is supersonic everywhere. In the earlier analyses, an inverse iteration method was used for the nose region, and the method of characteristics was employed for the remaining supersonic region. Both of these procedures are inferior from a computational point of view to more recently developed methods and were replaced in the modernization of these solutions described by Spreiter

and Stahara (1980a,b) and most comprehensively by Stahara et al. (1980). The nose region is treated using a new axisymmetric implicit unsteady Euler equation solver specifically developed for the present application. That procedure determines the solution in the nose region by an unsteady asymptotic time-marching procedure which advances the solution forward in time until the steady state is attained. The remainder of the flow field is determined by a shock capturing marching procedure which spatially advances the solution downstream as far as required by solving the steady Euler equations. Inasmuch as these methods are complex, lengthy, and fully described in the above references, we turn directly to a discussion of the results.

Figures 9 and 10 show typical results for the Earth for representative solar wind conditions of $\gamma = 5/3$ and $M_{S_\infty} = 8$. In addition to the bow wave and the magnetopause, Figure 9 shows the sonic line which delineates the boundary between subsonic and supersonic flow, the streamlines which indicate the local direction of the flow, and the Mach or characteristic lines which indicate the zones of influence and dependence of an infinitesimal disturbance in the flow. Figure 10 shows contour lines of constant density, velocity, and temperature. These are sharply defined solutions, with much finer resolution than the magnetohydrodynamic solutions presently available, and can be determined in one to two minutes on a large modern computer as opposed to several hours for a much less well resolved magnetohydrodynamic solution. An extensive catalog of results for various interplanetary conditions is given in Stahara et al. (1980).

With the flow field determined by the gasdynamic calculations, the magnetic field $\underset{\sim}{B}$ may be determined by integrating equations (14) and (26); or alternatively the following equations derived from them

$$\frac{D}{Dt} \int \int_S \underset{\sim}{B} \cdot d\underset{\sim}{S} = 0 \, , \quad \frac{D}{Dt} \left(\frac{\underset{\sim}{B}}{\rho} \right) = \frac{1}{\rho} \left(\underset{\sim}{B} \cdot \underset{\sim}{\nabla} \right) \underset{\sim}{v} \tag{35}$$

in which S is an arbitrary surface moving with the fluid and $D/Dt = \partial/\partial t + (\underset{\sim}{v} \cdot \underset{\sim}{\nabla})$ is the material or substantial derivative. As noted previously, these equations are commonly interpreted as indicating the field lines move with the fluid. For the steady state in which $\partial/\partial t = 0$ and $\tilde{v}_n = v_n$, these equations lead to a straightforward calculation in which the vector distance from each point on an arbitrarily selected field line to its corresponding point on an adjacent field line in the downstream direction is determined by numerically integrating $\int \underset{\sim}{v} \, dt = \Delta \underset{\sim}{s}$ over a fixed time interval Δt. Once the magnetic field lines are determined, the magnetic field at any point may be calculated from the relation

$$\underset{\sim}{B}/B_\infty = (\rho/\rho_\infty)(\Delta \underset{\sim}{\ell}/\Delta \ell_\infty) \tag{36}$$

where $\Delta \underset{\sim}{\ell}$ is the vector length of a small element of a flux tube. In closing this discussion, one should observe that, in general, both streamlines and magnetic field lines are three-dimensional curves. For axisymmetric flows, the streamlines are planar curves, but the field

lines are three-dimensional curves except for the special case of aligned field flow in which the $\underset{\sim}{B}$ and $\underset{\sim}{v}$ vectors are locally parallel throughout the flow.

The foregoing procedure is valid generally, but for axisymmetric flows it is much simpler and completely equivalent to compute the magnetic field by a decomposition theorem developed by Alksne and Webster (1970) whereby the magnetic field at P is given by

$$\underset{\sim}{B}_P = \left(\frac{\underset{\sim}{B}_P}{B_\infty}\right)_{\parallel} B_{\infty_{\parallel}} + \left(\frac{\underset{\sim}{B}_P}{B_\infty}\right)_{\perp} B_{\infty_{\perp}} + \hat{e}_n \left(\frac{B_P}{B_\infty}\right)_n B_{\infty_n} \tag{37}$$

in which

$$\left(\frac{\underset{\sim}{B}_P}{B_\infty}\right)_{\parallel} = \frac{\rho \underset{\sim}{v}_P}{\rho_\infty v_\infty} \quad , \quad \left(\frac{\underset{\sim}{B}_P}{B_\infty}\right)_n = \frac{r_p \rho_p}{r_{p_\infty} \rho_\infty} \tag{38}$$

can be calculated directly from the gasdynamic solution. $(\underset{\sim}{B}_P/B_\infty)_{\perp}$ must still be calculated using the $\Delta\underset{\sim}{s}$ - $\Delta\underset{\sim}{\ell}$ method, but only for the plane of magnetic symmetry in which $B_{\infty_n} = 0$ and for which $\underset{\sim}{B}_P$ is two-dimensional. In this decomposition, the subscripts $\parallel$, $\perp$, and n refer to contributions associated with the component $B_{\infty_{\parallel}}$ of $\underset{\sim}{B}_\infty$ parallel to $\underset{\sim}{v}_\infty$; the component $B_{\infty_{\perp}}$ perpendicular to $\underset{\sim}{v}_\infty$ in the plane that contains the point P, the center of the planet, and the vector $\underset{\sim}{v}_\infty$; and the component B_{∞_n} normal to the latter plane, where $\hat{e}_n$ is a unit vector in the latter direction. The quantity r_p in equation (38) is the radial cylindrical coordinate of the streamline through P. Figure 11 is included to facilitate understanding of the quantities involved in this analysis, a

key point of which is the orientation of the coordinate system so that the point P at which the magnetic field is to be evaluated is in the $x_\perp$ plane.

Representative results for the magnetic field direction and intensity are shown in Figure 12. The upper part of the figure presents the magnetic field lines and contours of equal field magnitude in the plane of magnetic symmetry, for which the magnetic field lines are all planar curves. Out of this plane, the field lines are three-dimensional curves and two projections are necessary to convey the results. These magnetic field results vary greatly with changes in the interplanetary field direction, but are relatively insensitive to moderate variations in the other flow parameters.

A property of the magnetic field calculated in this way that is sometimes cited as a deficiency of the theory, but which can actually be understood in terms of real processes as viewed in the limit of vanishing magnetic field and dissipation, is that the calculated field becomes very large near the magnetoionopause. This may be deduced directly from equation (36) for the general case or equations (37) and (38) for axisymmetric flows from the fact that $\underset{\sim}{B}_p\rho_\infty/(B_\infty\rho_p)$ approaches infinity as P approaches the magnetoionopause, because the length $\Delta\underset{\sim}{\ell}/\Delta\ell_\infty$ of the element of a convecting magnetic flux tube directly incident upon the magnetoionopause nose enlarges indefinitely as it flows past the magnetoionopause. It should be noted that this is not just for the gasdynamic-convected-field model, but applies equally to the dissipationless magnetohydrodynamic theory since equation (36) is an

exact relation in that theory. The only difference between the gasdynamic and magnetohydrodynamic procedures is the difference in the values for $\underset{\sim}{v}$ in the calculation of $\Delta\underset{\sim}{s} = \int \underset{\sim}{v}\, dt$. Such changes will invalidate the above statements only if $\underset{\sim}{v}$ is zero in the magnetohydrodynamic solution over the entire magnetoionopause instead of just at the stagnation point and that is not the case. The theory thus indicates that either $\underset{\sim}{B}_p/B_\infty$ is infinite or ρ_p is zero. Both possibilities are meaningful in the limit of vanishing dissipation and interplanetary field as we explain below.

If the boundary is of the pure magnetopause type with a vacuum magnetic field in the magnetosphere, the interpretation is that $\underset{\sim}{B}_p$ increases to the finite magnetospheric level, which is independent of the interplanetary field B_∞; and ρ diminishes to zero as the point P moves across the magnetopause from the solar wind plasma to the magnetosphere. Now the theory does not provide values for $\underset{\sim}{B}_p$ directly, but only for the ratio $\underset{\sim}{B}_p\rho_\infty/(B_\infty \rho_p)$ and that strictly only in the limit of vanishing B_∞. The infinite value for this ratio is thus the theory's best effort to predict a finite value for $\underset{\sim}{B}_p$ that is independent of B_∞ as B_∞ approaches zero. In the dissipationless magnetohydrodynamic theory for which the limiting process of vanishing B_∞ would not be applied, the magnetic field would be expected to rise to the magnetospheric level in much the same way as the point P approaches the magnetopause. Meanwhile the density would drop in such a solution and become exactly zero at the idealized magnetopause; so that in that interpretation of the theory $\underset{\sim}{B}_p\rho_\infty/(B_\infty\rho_p)$ becomes infinite at the magnetopause, but for a different reason. This is, in fact, the

mechanism by which a magnetopause would form in dissipationless magnetohydrodynamic theory with distinct magnetic field configurations on the two sides of the boundary for steady flows.

If, on the other hand, the boundary is of a pure ionopause type for which there may be no ionospheric magnetic field, the prediction of infinite $\underset{\sim}{B}_p \rho_\infty / (B_\infty \rho_p)$ may still be understood, although in a somewhat different way. As point P approaches the ionopause, the magnetic field would again rise, but this time the rise would be limited by the ionospheric pressure, which is independent of the interplanetary field. Thus the ratio of the finite ionopause magnetic field to the interplanetary magnetic field is infinite in the limit of vanishing interplanetary magnetic field. If the magnetic field actually rose to such a value as to balance the ionospheric pressure, the gas pressure would be driven toward zero. This would indicate the presence of magnetic barrier region of high field and little plasma separating the flowing solar wind and the ionospheric plasmas. From the higher point of view of dissipative theory, an ionopause is a shear layer in hypersonic flow in which intensive heating occurs. Since the pressure on the ionopause is determined primarily by the momentum balance and is nearly independent of the dissipative processes, a rise in temperature leads, through the perfect gas law $P = \rho R T/\overline{m}$, to a fall in density in the shear layer. In this way, a barrier region of hot rarefied plasma would form between the solar wind and the ionospheric plasma even in the absence of all magnetic fields. From several points of view, therefore,

it appears plausible to expect these theories to predict enhancement of the interplanetary magnetic field near a magnetoionopause and a relatively evacuated magnetic barrier region at an ionopause.

The above account provides an overview of the essential parts of the gasdynamic-convected-field model, and its relationship to the dissipative and nondissipative magnetohydrodynamic theories from which it is derived. Once the flow and magnetic field properties are determined in the manner described, further extensions such as to the calculation of the electric field $\underset{\sim}{E} = -(\underset{\sim}{v} \times \underset{\sim}{B})/c$, proton velocity distributions, and many other quantities can be accomplished in a straightforward way with the introduction of the appropriate formulae. Because it is the most completely worked out method for calculating planetary bow waves and their associated flow fields and is gaining widespread use in the interpretation and analysis of data, we feel it appropriate in concluding this section to make a number of general remarks about the present state of this theory as implemented by the computer model of Stahara et al. (1980), and Spreiter and Stahara (1980a,b).

First of all, it should be understood that the gasdynamic-convected-field model is essentially a magnetohydrodynamics theory in the limit-of vanishing dissipation and vanishing B_∞, i.e., for $M_{A_\infty} \to \infty$ with $M_A > M_S$. Numerical solutions are obtained after the introduction of additional approximations, particularly the Newtonian pressure relation and an axisymmetric obstacle shape. The entire model is fully implemented with a documented computer code in NASA CR 3182

(Stahara et al., 1980). An entire calculation requires about 120 seconds for a single case on a CDC 7600 or about 20 seconds on a Cray XMP. About 90 percent of this time is for the gasdynamic part of the calculation, with only about 10 percent being required for the magnetic field. The model is proving to be a useful tool in the interpretation of data, particularly in understanding effects of the three-dimensional nature of the interaction process. Several examples of this may be found in other articles in this conference proceedings. Extended applications currently underway include:

- bow shock shape and position for all the terrestrial planets (Slavin et al., 1981, 1983)

- distant planetary Mach cone and bow shock shapes for Venus, Earth and Mars (Slavin et al., 1984a)

- magnetospheric source of energetic particles upstream of Earth's bow shock (Luhmann et al., 1984b)

- locations and asymmetries of magnetic field merging sites on the Earth's magnetopause (Luhmann et al., 1984a; Crooker et al., 1984a)

- magnetic field draping on the Earth's magnetopause (Crooker et al., 1984b)

- intrinsic magnetic field of Mars (Russell, 1984)

- detailed plasma and field studies in the Venusian ionosheath (Mihalov et al., 1982)

- bow shock shape and position for Jupiter and Saturn (Slavin et al., 1984b)

CONCLUSIONS

To summarize the preceding discussion of magnetohydrodynamic and gasdynamic theories for planetary bow waves, we conclude with the following remarks.

Magnetohydrodynamic theory provides a good basis for modeling many aspects of planetary bow waves and their associated flow fields. Current development of numerical solutions for representative applications is in the early stages, and presently require extensive computer times. Even when these solutions are obtained, there remain a number of important phenomena that cannot be described by the theory. Examples include upstream waves or any other multi-component plasma process. Moreover, the dissipationless limit of the general MHD theory cannot account for any phenomena that depends on the finite thickness of shock waves, boundary layers, or current sheets.

The aligned magnetohydrodynamic case in which the magnetic field is aligned with the velocity can be reduced to a pseudogasdynamics problem

and solved by methods of gasdynamics. The results display substantial effects of variations of the Alfvén Mach number as well as the sonic Mach number, and are of such nature that they cannot be made into a function of one parameter by any combination of the sonic and Alfvénic Mach numbers.

The gasdynamic-convected-field theory is a limiting form of magnetohydrodynamic theory for large Alfvén Mach number and for Alfvén Mach numbers in excess of the sonic Mach number. With the aid of certain additional approximations including the Newtonian pressure relation for predetermining the magnetoionopause shape and the introduction of an axisymmetric magnetoionopause shape, the theory can be reduced to a form that is both amenable to efficient numerical solution and satisfactorily accurate for many purposes. This theory has been fully implemented in a readily available model that has been demonstrated to give useful results over a wide range of conditions. Several groups are now actively using the model in their work, developing further extensions and applications, and generally finding the results useful for both interpreting data and developing new insights.

Finally, we note that the dissipationless, gasdynamic-convected-field theory contains certain properties that are sometimes interpreted as false and without meaning, but which actually can be understood as true indicators of real processes when viewed in the limit of vanishing dissipation and interplanetary magnetic field. A discussion of several examples is provided.

ACKNOWLEDGEMENTS

The preparation of this paper was supported in part by the National Aeronautics and Space Administration under grant NAGW-2781 to Stanford University and by RM Associates, Inc., Independent Research and Development Program.

REFERENCES

Alksne, A. Y., The Steady-State Magnetic Field in the Transition Region Between the Magnetosphere and the Bow Wave. Planet. Space Sci., 15, 239-245, 1967.

Alksne, A. Y., and D. L. Webster, Magnetic and Electric Fields in the Magnetosheath. Planet. Space Sci., 18, 1203-1212, 1970.

Axford, W. I., The Interaction Between the Solar Wind and the Earth's Magnetosphere. J. Geophys. Res., 67, 3791-3796, 1962.

Beard, D. B., The Interaction of the Terrestrial Magnetic Field with the Solar Corpuscular Radiation. J. Geophys. Res., 65, 3559-3568, 1960.

Brackbill, J. V., Numerical Modeling of Magnetospheric Reconnection. Los Alamos National Laboratory preprint, LA-UR-82-483, 1982.

Briggs, B. R., and J. R. Spreiter, Theoretical Determination of the Boundary and Distortion of the Geomagnetic Field in a Steady Solar Wind. NASA TR T-178, 1963.

Chapman, D. R., Computational Aerodynamics Development and Outlook. AIAA J., 17, 1293-1313, 1979.

Chapman, S. and V. C. A. Ferraro, A New Theory of Magnetic Storms. Terrest. Magnetism Atmospheric Electricity, 36, 77-97, 171-186, 1931.

Crooker, N. V., J. G. Luhmann, J. R. Spreiter and S. S. Stahara, Characteristics of the Magnetospheric Source of Interplanetary Particles, J. Geophys. Res., in press, 1984a.

Crooker, N. V., J. G. Luhmann, C. T. Russell, E. J. Smith, J. R. Spreiter and S. S. Stahara, Magnetic Field Draping Against the Dayside Magnetopause, J. Geophys. Res., in press, 1984b.

Dryer, M. and R. Faye-Peterson, Magnetogasdynamic Boundary Conditions for a Self-Consistent Solution to the Closed Magnetopause. AIAA J., 4, 246-254, 1966.

Dryer, M. and G. R. Heckman, Application of the Hypersonic Analogy to the Standing Shock of Mars, Solar Physics, 2, 112-120, 1967.

Ferraro, V. C. A., On the Theory of the First Phase of a Geomagnetic Storm: A New Illustrative Calculation Based on an Idealized (Plane not Cylindrical) Model Field Distribution. J. Geophys. Res., 57, 15-49, 1952.

Jeffrey, A., Magnetohydrodynamics. Oliver and Boyd Ltd., Edinburgh, Scotland, 1966.

Jeffrey, A. and T. Taniuti, Non-Linear Wave Propagation. Academic Press, New York, 1964.

Kellogg, P. J., Flow of Plasma Around the Earth, J. Geophys. Res., 67, 3805 - 3811, 1962.

Landau, L. D. and E. M. Lifshitz, Electrodynamics of Continuous Media. Addison-Wesley Pub. Co. Reading, Mass., 1960.

Luhmann, J. G., R. J. Walker, C. T. Russell, N. U. Crooker, J. R. Spreiter and S. S. Stahara, Patterns of Magnetic Field Merging Sites on the Magnetopause, J. Geophys. Res., 89, 1739-1742, 1984a.

Luhmann, J. G., R. J. Walker, C. T. Russell, N. U. Crooker, J. R. Spreiter, S. S. Stahara and D. J. Williams, Characteristics of the Magnetospheric Source of Interplanetary Energetic Particles, J. Geophys. Res., in press, 1984b.

Mihalov, J. D., J. R. Spreiter and S. S. Stahara, Comparison of Gas Dynamic Model with Steady Solar Wind Flow Around Venus. J. Geophys. Res., 87, 10363-10371, 1982.

Russell, C. T., J. G. Luhmann, J. R. Spreiter and S. S. Stahara, The Magnetic Field of Mars: Implications from Gas Dynamic Modeling, J. Geophys. Res., 89, 2997-3003, 1984.

Slavin, J. A. and R. E. Holzer, Solar wind flow about the terrestrial planets, 1. Modeling bow shock position and shape, J. Geophys. Res., 86, 11,401-11,418, 1981.

Slavin, J. A., R. E. Holzer, J. R. Spreiter, S. S. Stahara and D. S. Chausee, Solar wind flow about the terrestrial planets, 2. Comparison with gas dynamic theory and implications for solar-planetary relations, J. Geophys. Res., 88, 19-35, 1983.

Slavin, J. A., R. E. Holzer, J. R. Spreiter and S. S. Stahara, Planetary Mach Cones: Theory and observations, J. Geophys. Res., 89, 2708-2714, 1984a.

Slavin, J. A., E. J. Smith, J. R. Spreiter and S. S. Stahara, Gasdynamic Modeling of the Jupiter and Saturn Bow Shocks; Solar Wind Flow About the Outer Planets, J. Geophys. Res., in press, 1984b.

Spreiter, J. R. and B. R. Briggs, Theoretical Determination of the Form of the Hollow Produced in a Solar Corpuscular Stream by the Interaction With the Magnetic Dipole Field of the Earth, NASA TR R-120, 1961.

Spreiter, J. R. and B. R. Briggs, Theoretical Determination of the Form of the Boundary of the Corpuscular Stream Produced by Interaction with the Magnetic Dipole Field of the Earth, J. Geophys. Res., 67, 37-51, 1962.

Spreiter, J. R. and W. P. Jones, On the Effect of a Weak Interplanetary Magnetic Field on the Interaction Between the Solar Wind and the Geomagnetic Field. J. Geophys. Res., 68, 3555-3564, 1963.

Spreiter, J. R., A. Y. Alksne and B. Abraham-Shrauner, Theoretical Proton Velocity Distribution in the Flow Around the Magnetosphere. Planet. Space Sci., 14, 1207-1220, 1966a.

Spreiter, J. R., A. L. Summers and A. Y. Alksne, Hydromagnetic Flow Around the Magnetosphere. Planet. Space Sci., 14, 223-253, 1966b.

Spreiter, J. R. and A. L. Summers, On Conditions Near the Neutral Points on the Magnetosphere Boundary. Planet. Space Sci., 15, 787-798, 1967.

Spreiter, J. R., A. Y. Alksne and A. L. Summers, External Aerodynamics of the Magnetosphere, in Physics of the Magnetosphere, R. L. Carovillano, J. F. McClay and H. R. Radoski (eds.), pp. 301-375, Reidel, Dordrecht, Holland, 1968.

Spreiter, J. R. and A. Y. Alksne, Plasma Flow Around the Magnetosphere. Revs Geophys., 7, 11-50, 1969.

Spreiter, J. R. and A. Y. Alksne, Solar-wind Flow Past Objects in the Solar System, in Annual Reviews of Fluid Mechanics, M. D. Van Dyke, W. G. Vincenti, and J. V. Wehausen (eds.), Vol. 2, 313-354, Annual Review, Palo Alto, CA, 1970a.

Spreiter, J. R., A. L. Summers and A. W. Rizzi, Solar Wind Flow Past Nonmagnetic Planets - Venus and Mars. Planet. Space Sci., 18, 1281-1299, 1970b.

Spreiter, J. R., M. C. Marsh, and A. L. Summers, Hydromagnetic Aspects of Solar Wind Flow Past the Moon. Cosmic Electrodynamics, 1, 5-50, 1970.

Spreiter, J. R. and A. W. Rizzi, Aligned Magnetohydrodynamic Solution for Solar Wind Flow Past the Earth's Magnetosphere, Acta Astronautica, 1, 15-35, 1974.

Spreiter, J. R., Magnetohydrodynamic and Gasdynamic Aspects of Solar-Wind Flow Around Terrestrial Planets - A Critical Review. NASA SP-397, 1976.

Spreiter, J. R. and S. S. Stahara, A New Predictive Model for Determining Solar Wind-Terrestrial Planet Interactions. J. Geophys. Res., 85, 6769-6777, 1980a.

Spreiter, J. R. and S. S. Stahara, Solar Wind Flow Past Venus: Theory and Comparisons. J. Geophys. Res., 85, 7715-7738, 1980b.

Stahara, S. S., D. Klenke, B. C. Trudinger and J. R. Spreiter, Application of Advanced Computational Procedures for Modeling Solar-Wind Interactions with Venus - Theory and Code. NASA CR 3267, 1980.

Walters, G. K., On the Existence of a Second Standing Shock Attached to the Magnetosphere. J. Geophys. Res., 71, 1341-1344, 1966.

Walker, R. J., Modeling Planetary Magnetospheres. Revs. Geophys. Space Phys., 21, 495-507, 1983.

Wu, C. C., R. J. Walker and J. M. Dawson, A Three Dimensional MHD Model of the Earth's Magnetosphere, Geophysical Res. Letters, 8, 523-526, 1981.

Wu, Z. J. and K. D. Cole, The Ratio Between Magnetotail Height and Neutral Point Height. Planet Space Sci., 30, 711-713, 1982.

Wu, C. C., Shape of the Magnetosphere. Geophys. Res. Letters, 10, 545-548, 1983.

FIGURE CAPTIONS

Figure 1. Illustration of solar wind flows past major bodies in the solar system.

Figure 2. Two-dimensional magnetohydrodynamic simulation of evolution of the geomagnetic field in a substream (Brackbill, 1982).

Figure 3. Magnetohydrodynamic propagation speeds for plane waves.

Figure 4. Magnetohydrodynamic Mach cone traces delineating regions of influence of a small disturbance at a fixed point in a steady flow.

Figure 5. Calculated bow wave positions for various Alfvén Mach numbers M_{A_∞} in a steady aligned magnetohydrodynamic flow with $M_{S_\infty}=10$ and $\gamma=5/3$ (Spreiter and Rizzi, 1974).

Figure 6. Results of three-dimensional magnetohydrodynamic simulation of steady solar wind flow past the dipole magnetic field of the Earth in the absence of an interplanetary magnetic field (Wu et al., 1981).

Figure 7. Shape and size of the Earth's magnetopause according to the Chapman-Ferraro theory, or equivalently the Newtonian gasdynamic model.

Figure 8. Outline of two alternative methods for calculating axisymmetric supersonic flow past a blunt-nosed body.

Figure 9. Calculated gasdynamic streamlines and Mach lines for steady supersonic solar wind flow past the Earth's magnetosphere, $M_{S_\infty}=8$, $\gamma=5/3$.

Figure 10. Calculated gasdynamic density, velocity, and temperature contours for steady supersonic solar wind flow past the Earth's magnetosphere, $M_{S_\infty}=8$, $\gamma=5/3$.

Figure 11. Diagrams to illustrate the $x_{\perp n}$ coordinates and magnetic field components used in Equations (37) and (38) to implement the Alksne-Webster, (1970) magnetic field decomposition theorem for axisymmetric flows.

Figure 12. Magnetosheath magnetic field magnitude and direction for representative conditions for solar wind flow past the Earth, $M_{S_\infty}=8$, $\gamma=5/3$.

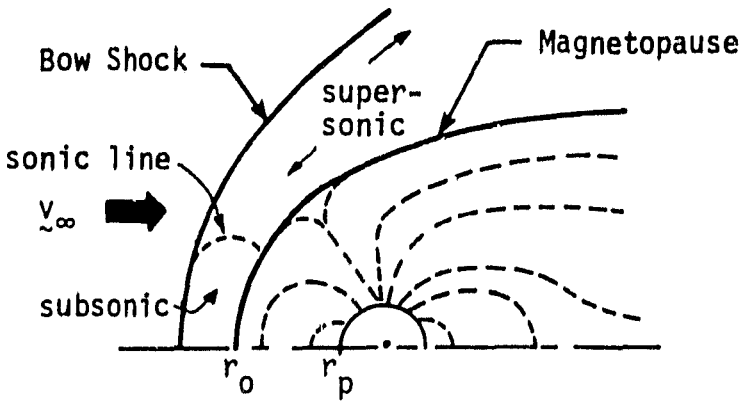

Magnetic Obstacles

Planet	r_p, k_m	r_o/r_p
Mercury	2400	1.5
Earth	6400	10.0
Mars (?)	3400	1.1
Jupiter	71000	70.0
Saturn	60000	22.0

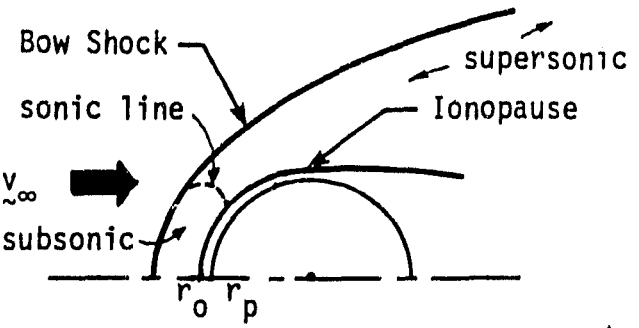

Ionospheric Obstacles

Planet	r_p, k_m
Venus	6200
Mars (?)	3400

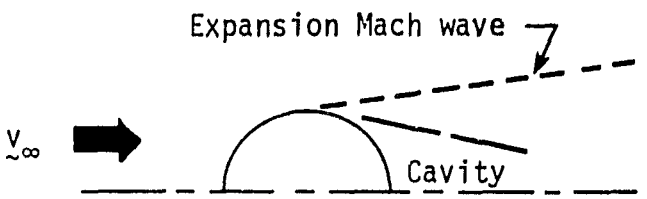

Solid Obstacles

	r_m, k_m
Moon	1700

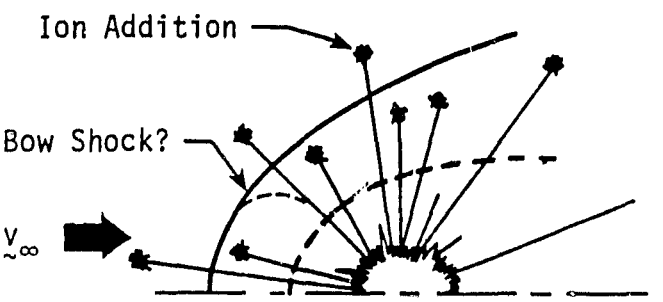

Cometary Obstacles

Large variety of sizes

FIGURE 1

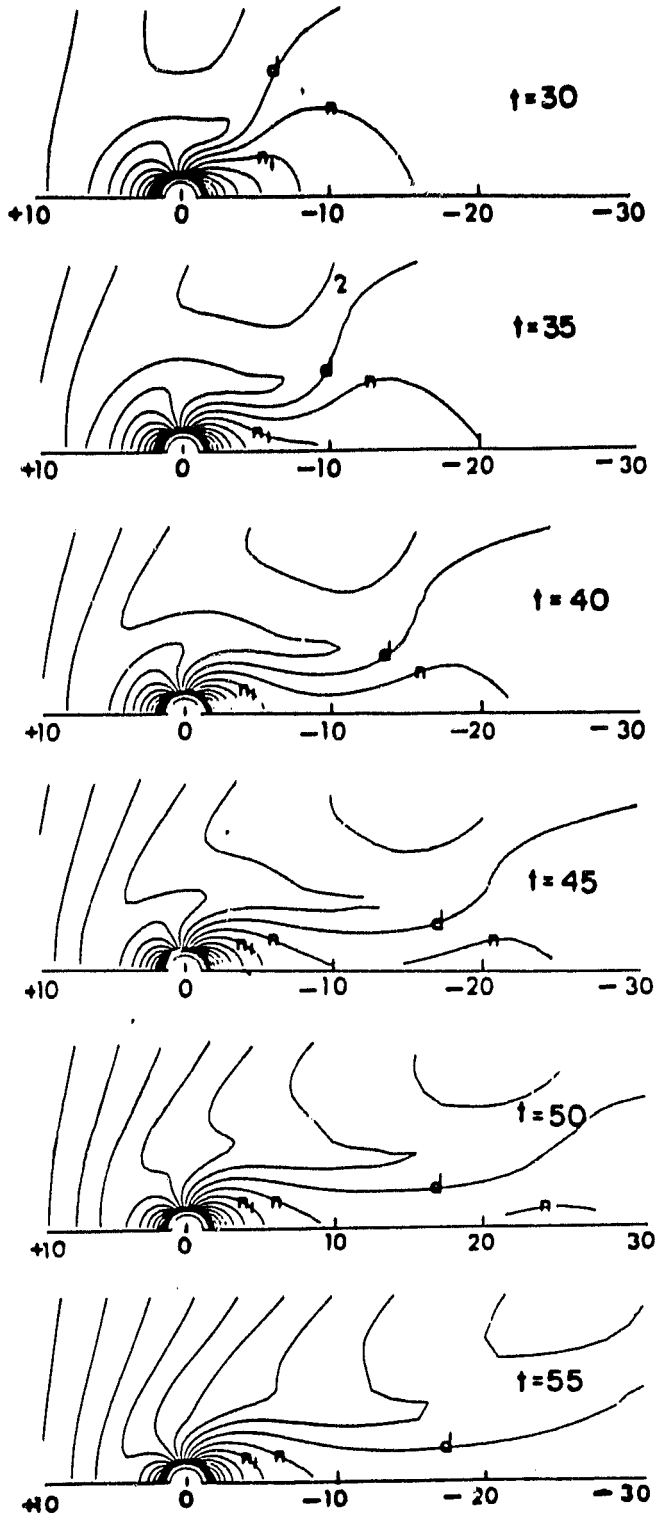
t=30
+10
0
-10
-20
-30
2
t=35
+10
0
-10
-20
-30
t=40
+10
0
-10
-20
-30
t=45
+10
0
-10
-20
-30
t=50
+10
0
10
20
30
t=55
+10
0
-10
-20
-30

FIGURE 2

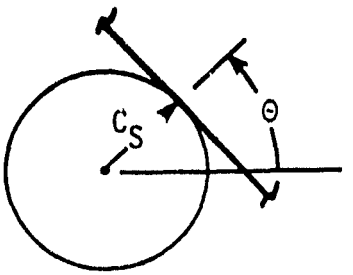

$\underset{\sim}{B} = 0$, GD Sound Wave

$C_S = \sqrt{\gamma RT/\bar{m}}$

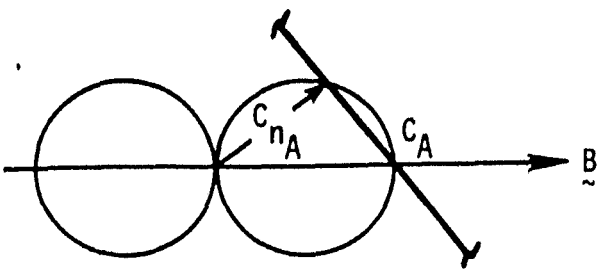

ρ = Const., MHD Alfvén Wave

$C_A = B/\sqrt{4\pi\rho}$

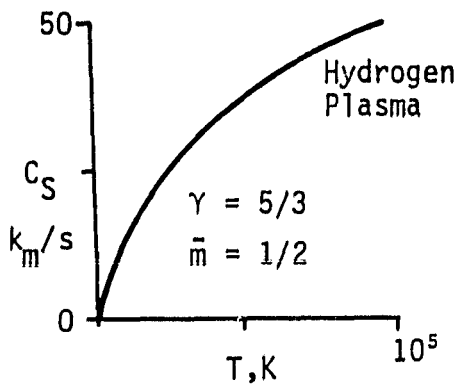

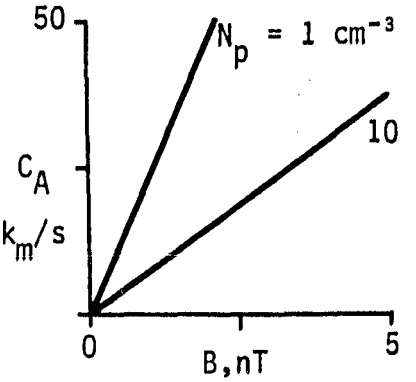

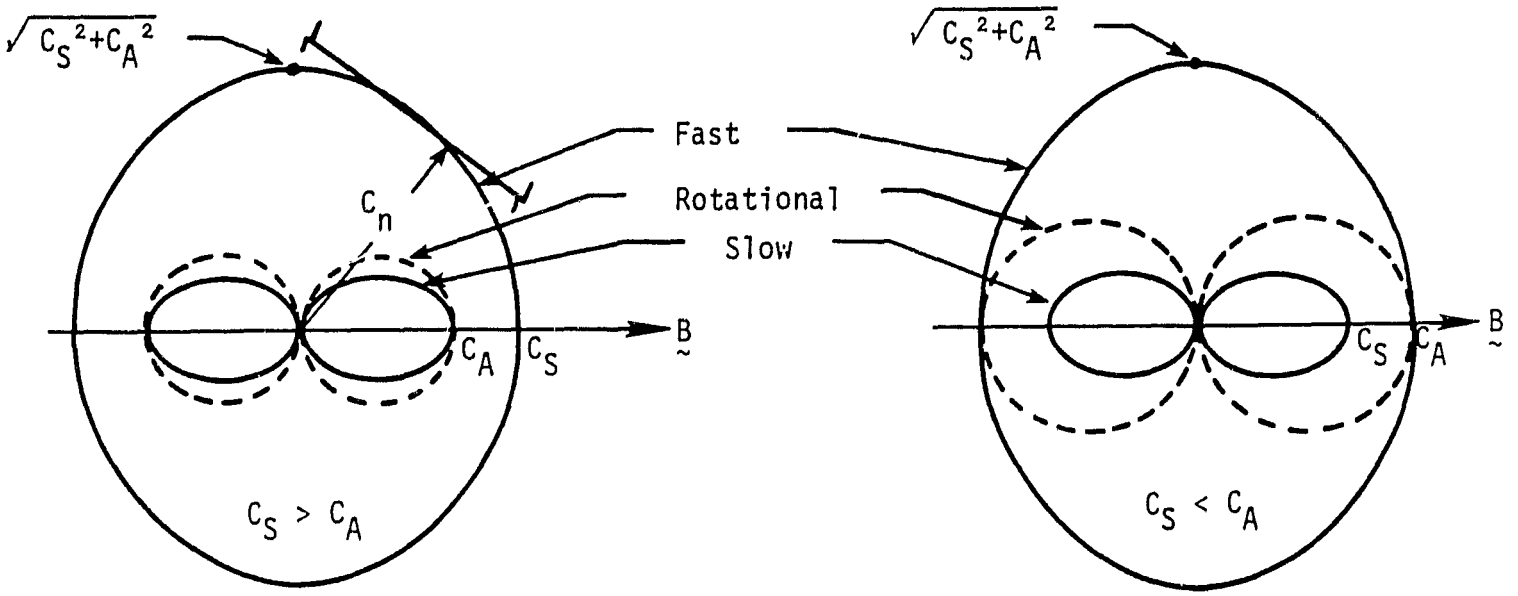

FIGURE 3

General MHD

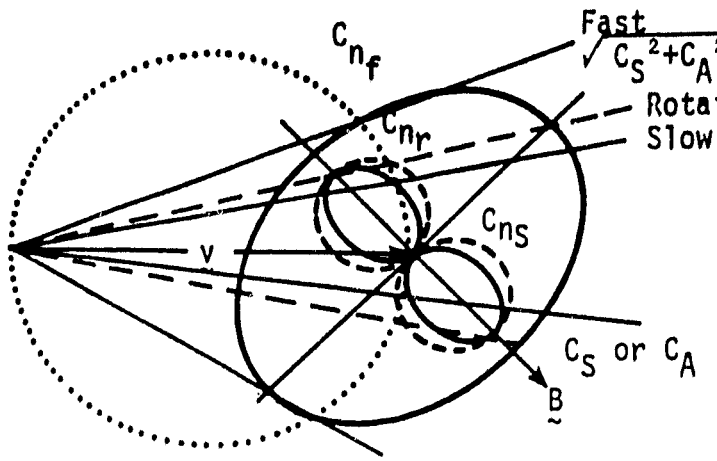

$\sin \omega = v_n/v$

Lim MHD = GD
B→0

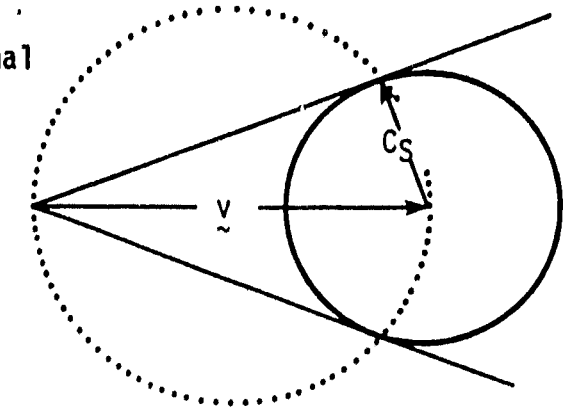

$\sin \omega_{GD} = C_S/v = M_S^{-1}$

Max Angle

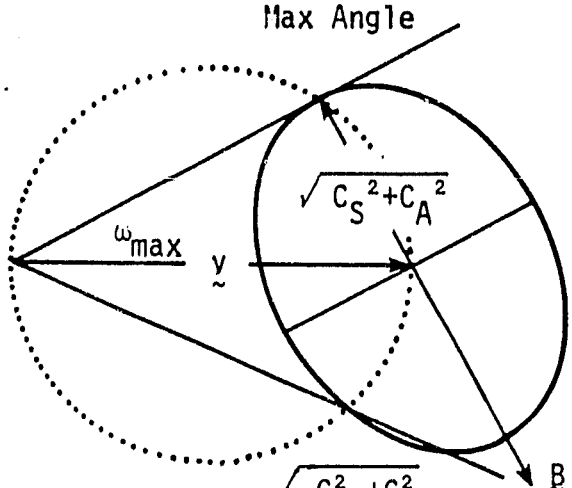

$$\sin \omega_{max} = \sqrt{\frac{C_S^2+C_A^2}{v^2}} = \sqrt{M_S^{-2}+M_A^{-2}}$$

Min Angle

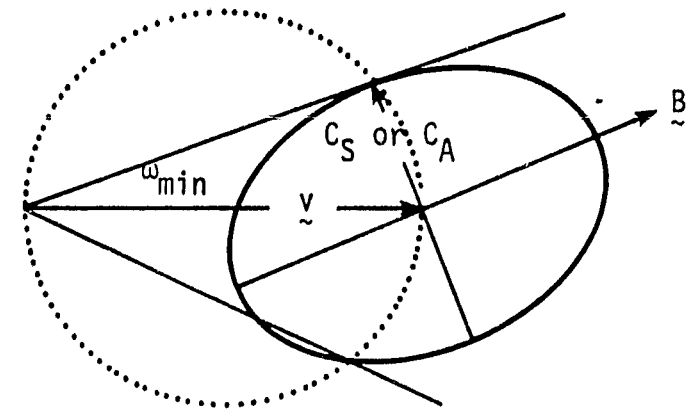

$\sin \omega_{min} = \max (M_S^{-1}, M_A^{-1})$

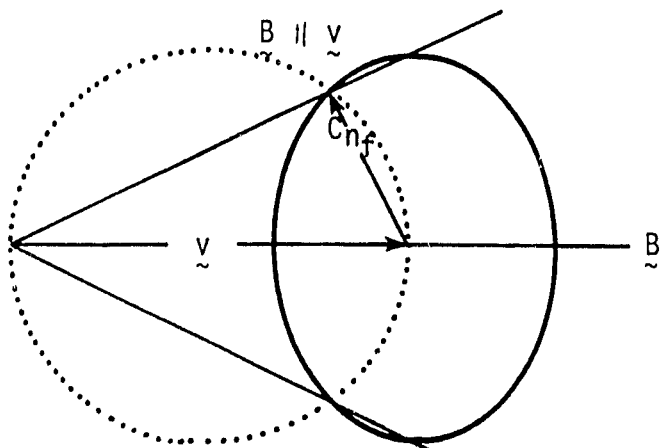

$$\sin \omega = \sqrt{\frac{M_S^2+M_A^2-1}{M_S^2+M_A^2}}$$

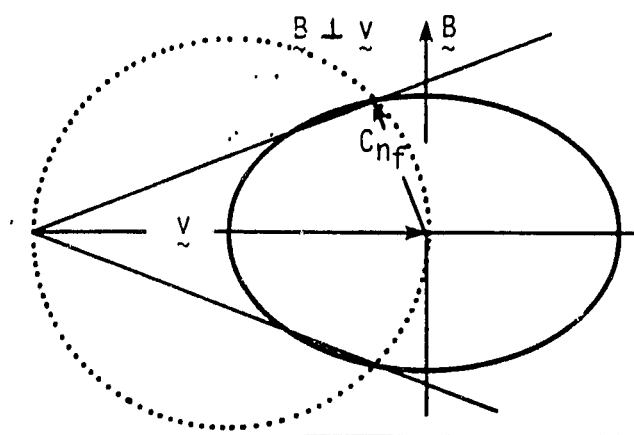

$$\sin \omega = \sqrt{\frac{M_S^2+M_A^2+1\pm\sqrt{(M_S^2+M_A^2+1)^2-4M_S^2M_A^2}}{2M_S^2M_A^2}}$$

FIGURE 4

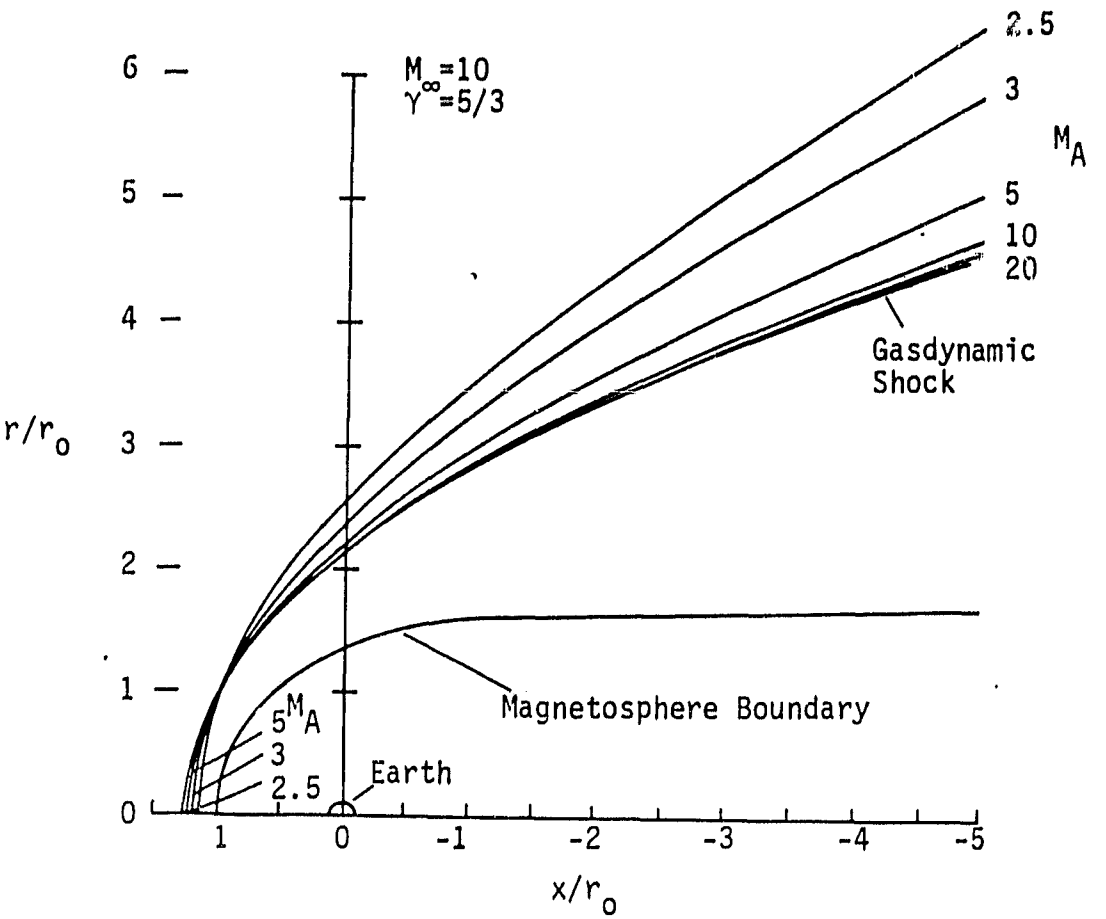
M_∞=10
γ^∞=5/3
2.5
3
5
10
20
M_A
Gasdynamic Shock
Magnetosphere Boundary
5
3
2.5
M_A
Earth
r/r_o
x/r_o
6
5
4
3
2
1
0
1
0
-1
-2
-3
-4
-5

FIGURE 5

DENSITY CONTOURS

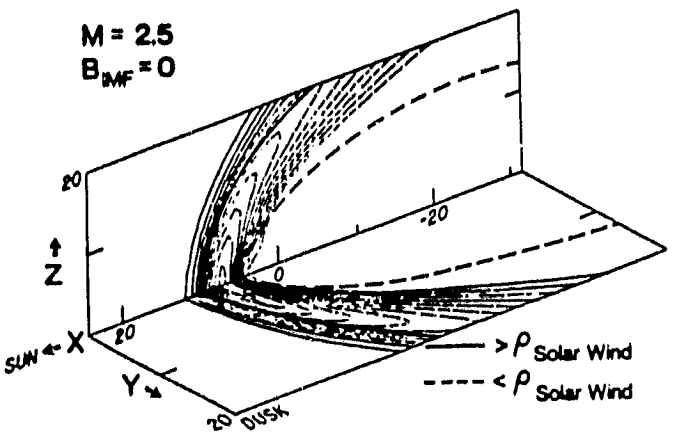

PRESSURE CONTOURS

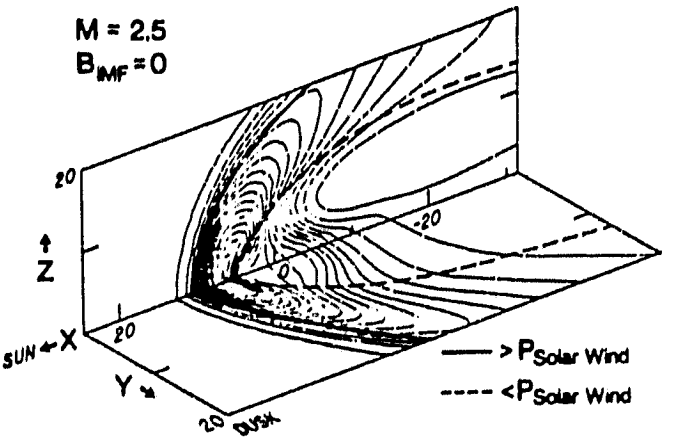

CONDITIONS ALONG SUN-EARTH LINE

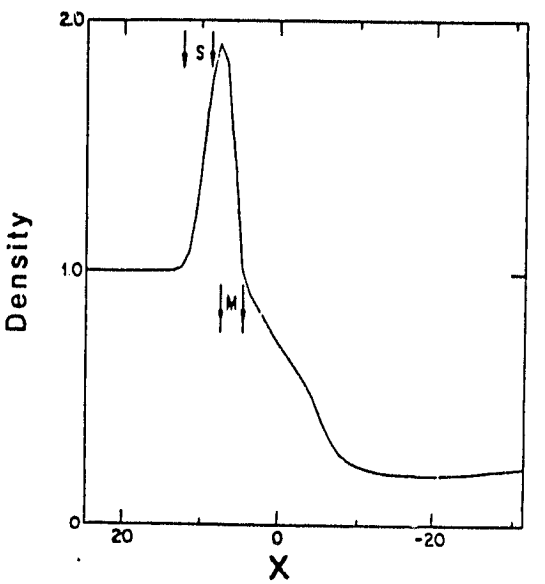

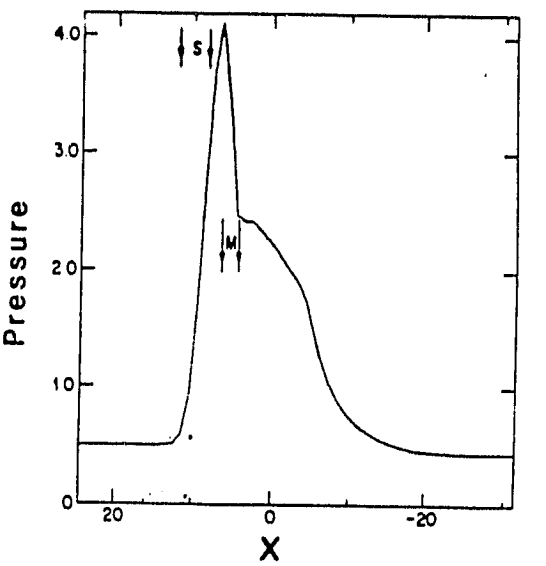

FIGURE 6

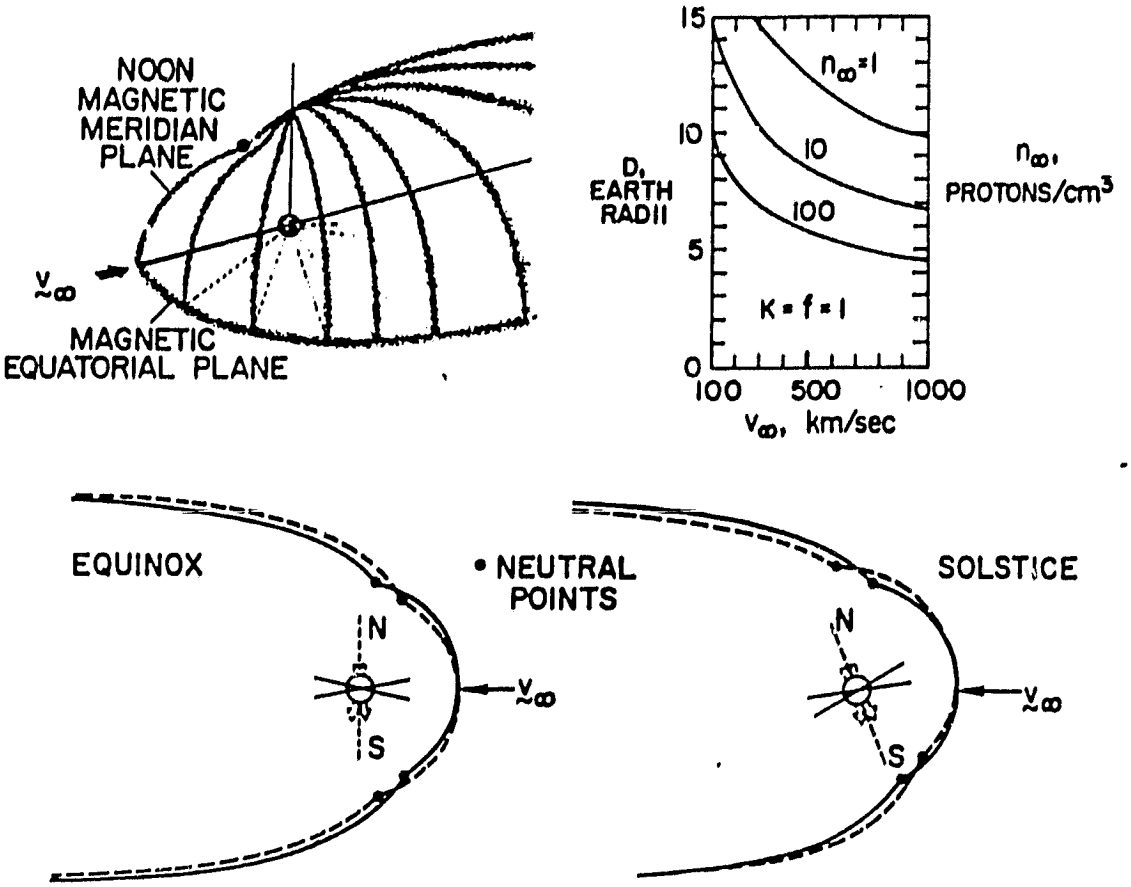
NOON
MAGNETIC
MERIDIAN
PLANE
v_∞
MAGNETIC
EQUATORIAL PLANE
15
10
5
0
D,
EARTH
RADII
n_∞=1
10
100
K = f = 1
100
500
1000
v_∞, km/sec
n_∞,
PROTONS/cm^3
EQUINOX
• NEUTRAL
POINTS
SOLSTICE
N
S
v_∞
N
S
v_∞

FIGURE 7

Former method

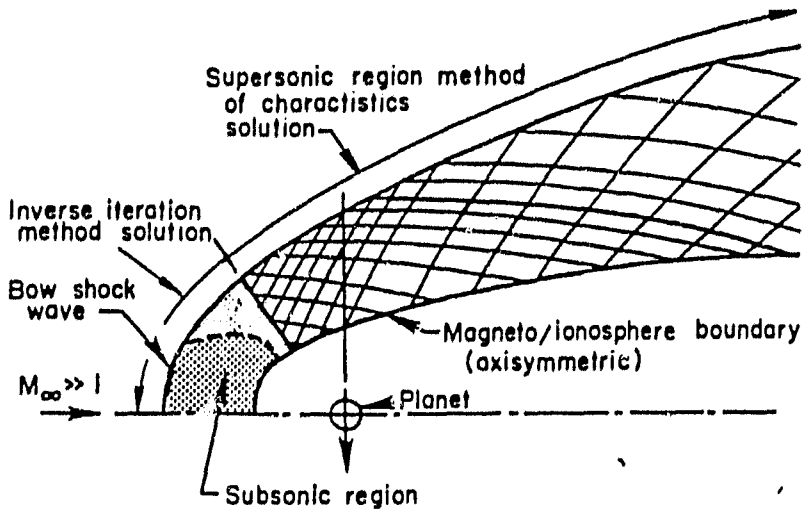

Present method

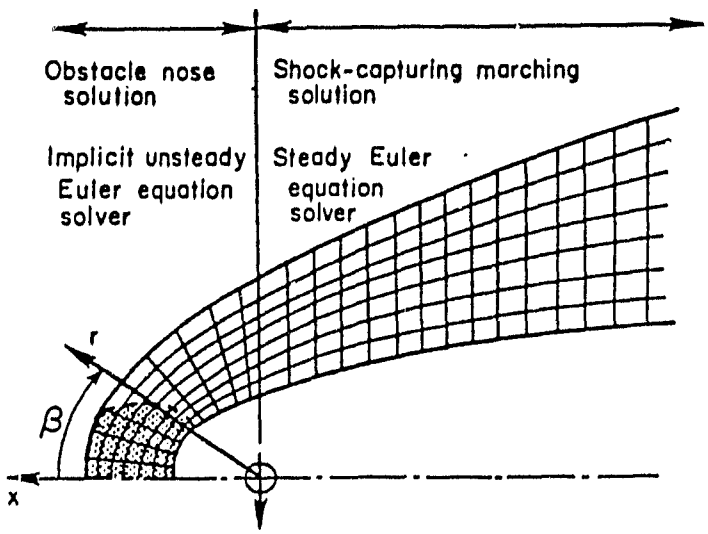

FIGURE 8

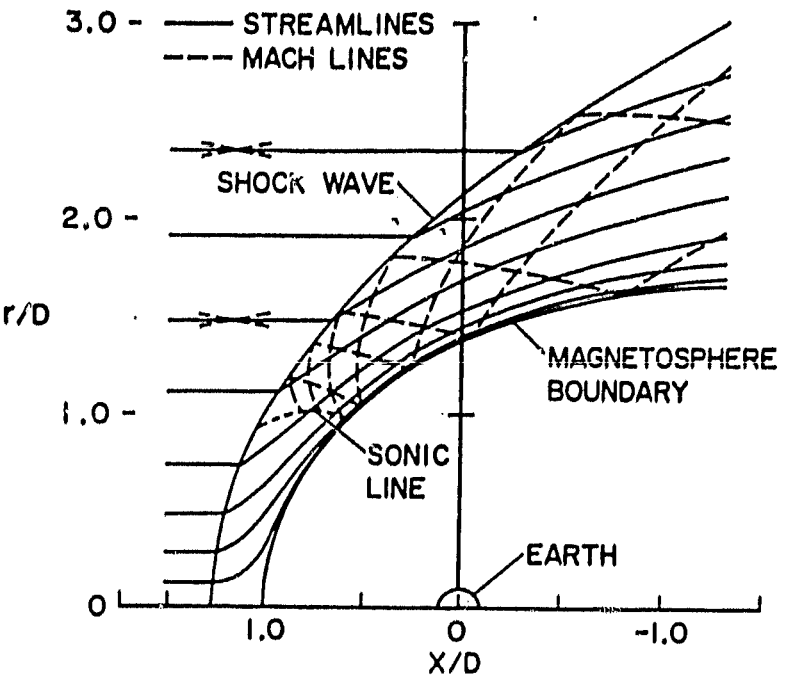
3.0
STREAMLINES
MACH LINES
SHOCK WAVE
2.0
r/D
MAGNETOSPHERE
BOUNDARY
1.0
SONIC
LINE
EARTH
0
1.0
0
-1.0
X/D

FIGURE 9

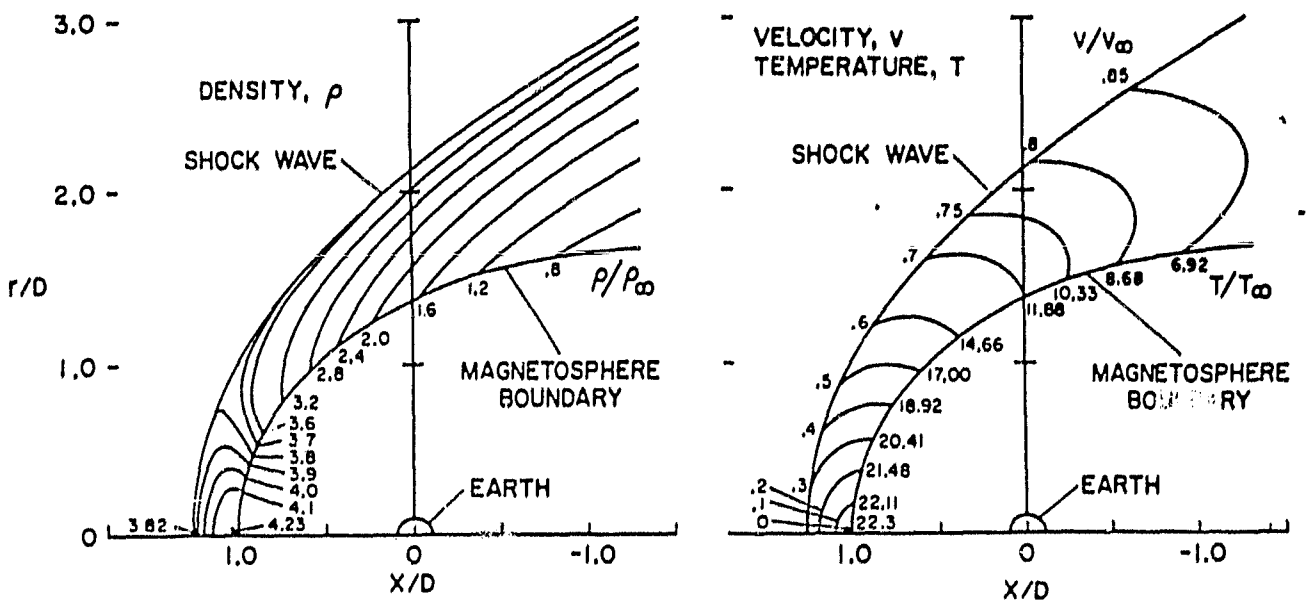
DENSITY, ρ
SHOCK WAVE
MAGNETOSPHERE BOUNDARY
EARTH
ρ/ρ∞
r/D
X/D
VELOCITY, V
TEMPERATURE, T
V/V∞
T/T∞
3.0
2.0
1.0
0
1.0
-1.0

FIGURE 10

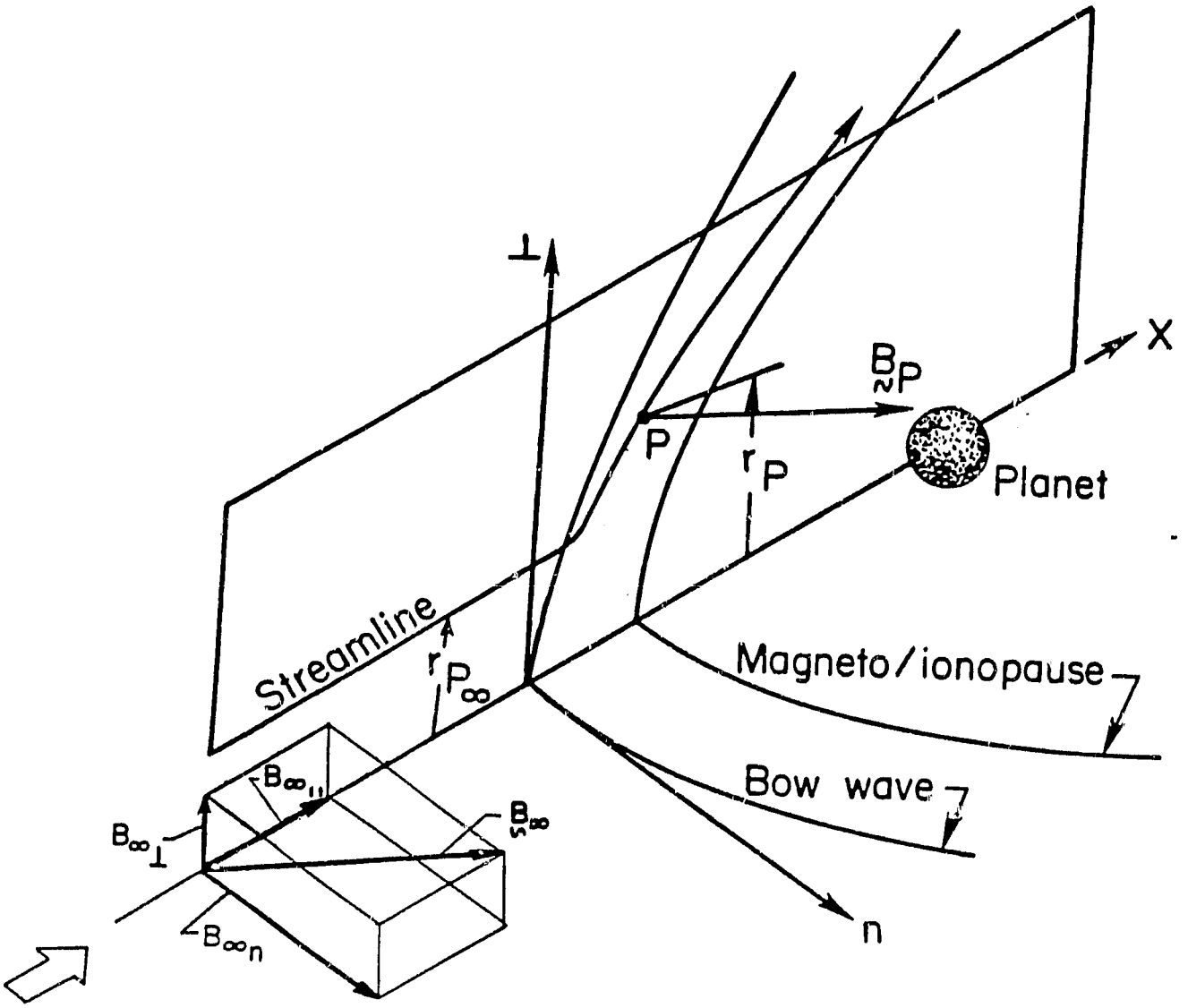
⊥
X
B_{NP}
P
r_P
Planet
Streamline
r_{P_∞}
Magneto/ionopause
Bow wave
$B_{\infty_\parallel}$
$B_{\infty_\perp}$
$B_{S\infty}$
B_{∞_n}
n

FIGURE 11

In Plane of Magnetic Symmetry

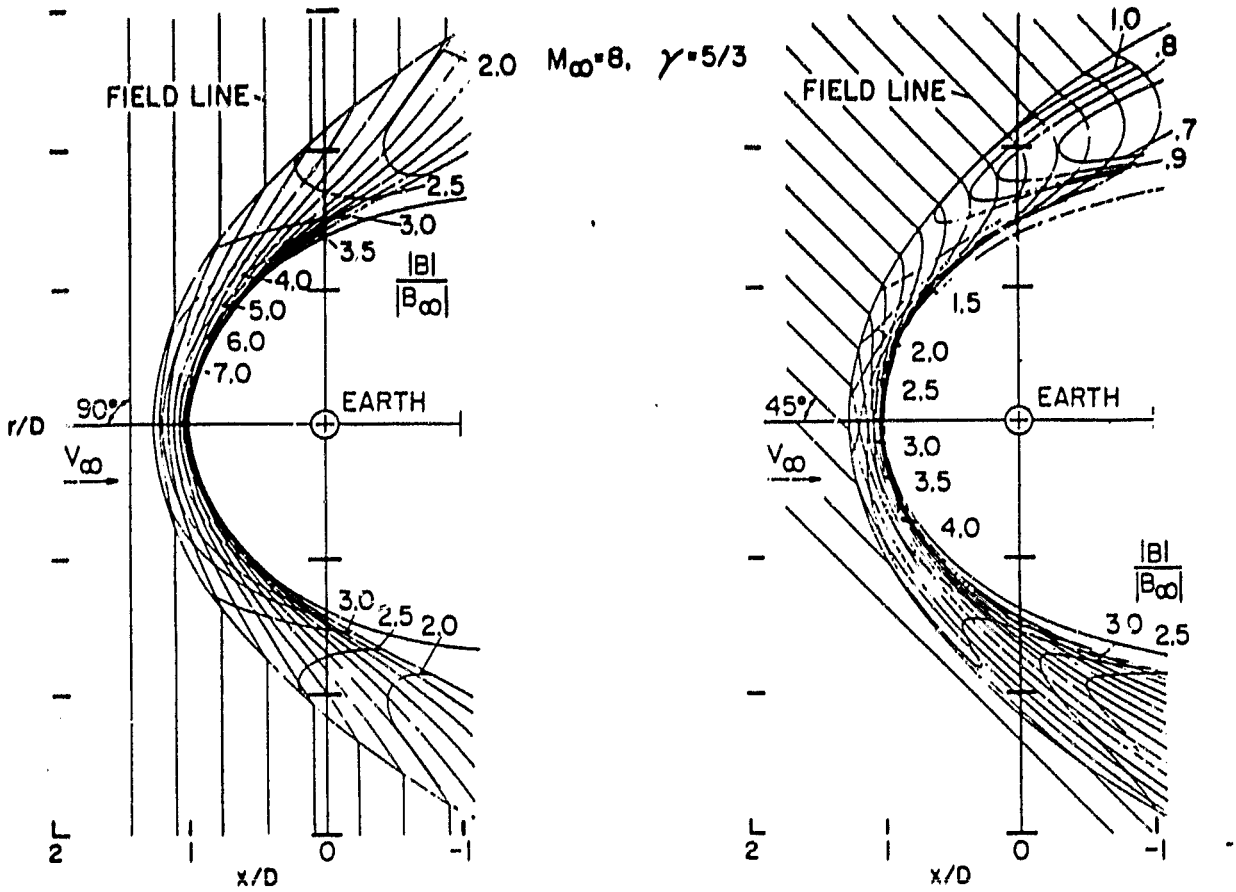

Out of Plane of Magnetic Symmetry

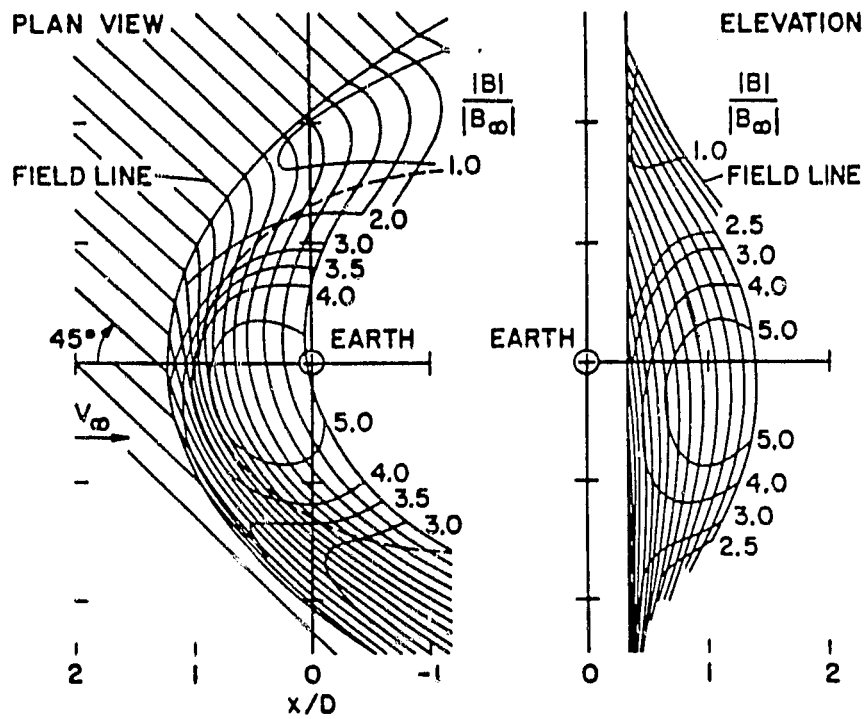

FIGURE 12